The University of British Columbia

Faculty of Graduate Studies

PROGRAMME OF THE

FINAL ORAL EXAMINATION
FOR THE DEGREE OF
DOCTOR OF PHILOSOPHY

of

JOHN EDWARDS MAYHOOD

B.Sc., Alberta
M.Sc., Alberta

•

MONDAY, MARCH 18th, 1957, at 2:30 p.m.

IN ROOM 300, PHYSICS BUILDING

COMMITTEE IN CHARGE

DEAN G. M. SHRUM, *Chairman*

A. M. CROOKER	C. A. MCDOWELL
J. B. WARREN	C. REID
M. BLOOM	R. H. WRIGHT
J. M. DANIELS	K. F. ARGUE

External Examiner — S. R. POLO
National Research Council

INTENSITY STUDIES IN THE INFRARED SPECTRA OF SULFUR DIOXIDE AND CARBON DISULFIDE

Abstract

The intensity of an infrared absorption band is determined by the change in the electric dipole moment of the molecule which accompanies the transition from the ground state to the excited vibrational state. Where the geometry of the molecule and its potential function are known, measured intensities may be used to calculate the moment changes associated with particular distortions of the molecule. Information on the internal redistribution of charge in a chemical bond when the bond is deformed can then be deduced if certain assumptions hold.

Measurements have been made on the integrated absorption coefficients of the three fundamental vibration-rotation bands of sulfur dioxide vapor. In contrast to previously reported values of these intensities, they yield a value of the molecular dipole moment which agress with the static dipole moment determined by other methods. The magnitudes of the moment changes found from the intensities are not consistent with the assumptions used in calculating them, indicating that the molecular model commonly used is not adequate. The discrepancies have been discussed in terms of the possible contributions of unshared electrons.

The frequencies, shapes, and intensities of infrared absorption bands differ markedly in the liquid and solid states from their values in the vapor state, due to the effects of collisions and intermolecular forces. Observations of these effects have been made for some absorption bands of sulfur dioxide and carbon disulfide. The results are not consistent with the predictions of the theory of dielectric polarization, nor with expectations based on simple collision theory. Such studies appear to offer a promising approach to information on intermolecular forces.

PUBLICATIONS

Some Correlations of the Molecular Structure of Organic Phosphorus Compounds with their Infrared Spectra:

R. B. Harvey and J. E. Mayhood,
Canad. J. Chemistry **33**: 1552-1565. (1955).

Classified Reports (Defence Research Board)

Suffield Technical Paper No. 13 — J. E. Mayhood and G. O. Langstroth (1952).
Suffield Technical Paper No. 35 — J. E. Mayhood (1954)
Suffield Technical Paper No. 61 — J. E. Mayhood and R. B. Harvey (1955).

GRADUATE STUDIES

Field of Study: Physics.

Electromagnetic Theory	W. Opechowski
Nuclear Physics	K. C. Mann
Quantum Mechanics	G. M. Volkoff
Molecular Spectroscopy	O. Theimer
Spectroscopy	A. M. Crooker and C. Cumming
Chemical Physics	J. S. Blakemore

Other Studies:

Theory of the Chemical Bond	C. Reid
Physical Organic Chemistry	C. C. Lee
Physical Chemistry	J. G. Hooley and C. Reid
Chemical Kinetics	W. A. Bryce

INTENSITY STUDIES IN THE INFRARED SPECTRA OF SULFUR DIOXIDE AND CARBON DISULFIDE

by

JOHN EDWARDS MAYHOOD

A THESIS SUBMITTED IN PARTIAL FULFILLMENT OF
THE REQUIREMENTS FOR THE DEGREE OF
DOCTOR OF PHILOSOPHY
in the Department
of
Physics

We accept this thesis as conforming to the standard required from candidates for the degree of DOCTOR OF PHILOSOPHY

Members of the Department of Physics

THE UNIVERSITY OF BRITISH COLUMBIA

March 1957

ABSTRACT

Measurements have been made of the integrated absorption coefficients of the three fundamental vibration-rotation bands of sulfur dioxide vapor. In contrast to previously reported values of these intensities, the molecular dipole moment calculated from them differs widely from the static dipole moment determined by other methods. The magnitudes of the bond moment derivatives are not in agreement with simple molecular models, indicating that infrared intensities are sensitive to the details of the electrical charge redistribution accompanying molecular distortions. The possible role of unshared electrons is discussed.

Observations on the shapes, frequencies, bandwidths, and intensities of some absorption bands of sulfur dioxide and carbon disulfide in condensed phases are reported and discussed in terms of the information they may give on intermolecular interactions.

In presenting this thesis in partial fulfilment of the requirements for an advanced degree at the University of British Columbia, I agree that the Library shall make it freely available for reference and study. I further agree that permission for extensive copying of this thesis for scholarly purposes may be granted by the Head of my Department or by his representative. It is understood that copying or publication of this thesis for financial gain shall not be allowed without my written permission.

Department of Physics

The University of British Columbia,
Vancouver 8, Canada.

Date Mar 10/67

ACKNOWLEDGMENTS

It is a pleasure to acknowledge the generous assistance received in the course of this work. Professor A.M. Crooker directed the research. The Defence Research Board provided financial support. The British Columbia Research Council made available its double-beam spectrometer, for which thanks are due to the Director, Dr. G.M. Shrum, and to Dr. R.H. Wright, Head of the Chemistry Division. Thanks are also due to Dr. J.D.H. Strickland and Mr. Trevor Clark of the British Columbia Research Council for advice and assistance on quantitative analysis. Dr. W.A. Bryce and Dr. J. Fabian of the Chemistry Department performed the mass spectrometric analysis. Finally, no work of this kind proceeds far without the technical assistance which can be given only by such experienced men as those who staff the shop facilities of the Department of Physics. To them, most particularly to Mr. John Lees, my most sincere thanks are extended.

Finally, I would like to give special acknowledgment to my wife, Barbara Mayhood, for constant support and encouragement, and for typing and proof-reading the thesis.

TABLE OF CONTENTS

TABLE OF TABLES

TABLE OF FIGURES

INTENSITY STUDIES IN THE INFRARED SPECTRA OF SULFUR DIOXIDE AND CARBON DISULFIDE

CHAPTER I

INTRODUCTION

The intensity of an infrared absorption band is determined by the change in the electric dipole moment of the absorbing molecule which accompanies the transition between the initial and final energy states.

In recent years there has been much interest in using measured infrared intensities to calculate the electric moment changes associated with absorption bands, and in attempting to relate these quantities to the internal structure and chemical behavior of molecules. Early efforts in this direction were hampered by the instability and low resolution of infrared spectrometers, by the absence of suitable computational procedures for treating polyatomic molecules, and by the scarcity of data on the potential functions of polyatomic molecules. These three deficiencies have been met with increasing success since about 1947, beginning with the publication of computational methods by Wilson (70), and of techniques for overcoming the effects of finite resolving power by Wilson and Wells (71). The historical development of intensity measurements up to 1954 has been reviewed by Vincent-Geisse (61, 62). Potential constants for polyatomic molecules are now being supplied by a combination of methods to which the

microwave spectrum is an important recent addition (32, 43).

The status of attempts to relate infrared intensities to the internal structure of molecules is somewhat uncertain. Hornig and McKean (26) have examined critically all the published data of this kind up to the end of 1954, and have pointed out the many inconsistencies and errors which may arise. It seems clear from their conclusions that the sensitivity of infrared intensities to the details of the internal charge distribution in a molecule gives considerable importance to intensity measurements as a tool in the study of molecules.

A further field of application for infrared intensities arises from the above considerations. The bulk properties of matter are derived from the intermolecular interactions, so that much interest attaches to the study of the perturbation of a molecule by its neighbors. It is reasonable to expect that the observed changes in intensity between molecules in the low-pressure gas phase and the high-pressure or condensed phases will give considerable information about intermolecular interactions. The excellent studies by such groups as those associated with Welsh (63, 64, 65), West (66, 67), and Ketelaar (20, 21, 24, 31) indicate the directions which are open for investigation in this connection.

The work to be reported in this thesis consists of two parts: (a) a contribution to the study of internal molecular structures, by way of measurements of the absolute intensities of the vibration-rotation bands of gaseous sulfur dioxide; (b) a contribution to the study of intermolecular forces, by way of observations on the spectrum of sulfur

dioxide in the liquid and solid phases, and on solutions of carbon disulfide and sulfur dioxide in organic solvents.

CHAPTER II

THEORETICAL CONSIDERATIONS

In order to provide notation and definitions needed in discussing the results, this section summarizes the relevant assumptions and equations underlying the measurements and the computations made from them. The bulk of the material is drawn from standard texts (76, 81) and recent literature.

1 The Intensities of Vibration-Rotation Bands

When a spectrometer of infinite resolving power is set at frequency ν, it records the intensity I, transmitted through an absorption cell of length ℓ containing a concentration C of absorbing molecules. Lambert's law then defines the absorption coefficient k_ν as

$$k_\nu = \frac{1}{C\ell} \ln \frac{I_o}{I}$$

where I_o is the intensity passed by the empty cell. The integral of the absorption coefficient across the whole frequency range of the i^{th} absorption band is called the integrated absorption coefficient or absolute intensity of the band, denoted by

$$A_i = \int_{\text{Band}} k_\nu \, d\nu = \frac{1}{C\ell} \int_{\text{Band}} \ln \frac{I_o}{I} \, d\nu \qquad (1)$$

This quantity may be related to the sum over all the allowed rotational transitions in a vibration-rotation band of the Einstein transition probability for absorption, which can in turn be expressed in terms of

the matrix elements of the total molecular dipole moment between the initial and final vibrational energy levels. It is necessary to assume that the vibrational and rotational energies are of different orders of magnitude and thus separable, and that the vibrational wavefunctions of both initial and final states can be written as the product of simple harmonic oscillator wavefunctions, one for each normal mode of vibration. The result, for a non-degenerate fundamental of the type $v'_k = v''_k + 1$, $v'_\ell = v''_\ell$ for $\ell \neq k$, is

$$\int_{\text{Band}} k_\nu \, d\nu = \frac{N\pi}{3c} \left[(\mu_x^k)^2 + (\mu_y^k)^2 + (\mu_z^k)^2 \right] \qquad (2)$$

where

$$\mu_x^k = \int \psi^*_{v'_k} \, \mu_x \, \psi_{v''_k} \, d\tau \qquad (3)$$

N = number of molecules per cc

c = velocity of light

ν = frequency in sec^{-1}.

The normal vibrations of a molecule define a set of "normal coordinates", Q_k, in terms of which each fundamental is a function of a single coordinate only. If the dipole moment components are expanded in terms of these coordinates,

$$\mu_x = \mu_x^\circ + \sum_{k=1}^{3N-6} \mu_x^k \cdot Q_k + \text{higher terms} \qquad (4)$$

and the assumption is made that the higher terms are small, then Equation (2) may be written

$$\int_{\text{Band}} k_\nu \, d\nu = \frac{N\pi}{3c} \left(\frac{\partial \vec{\mu}}{\partial Q_k} \right)^2 \qquad (5)$$

since Equation (3) essentially defines the change in the cartesian

component of the molecular dipole moment between the vibrationless groundstate (initial) and the final state in which the vibrational distortion is specified by the normal coordinate Q_k, i.e., $\partial\mu_x/\partial Q_k$. The observed intensities thus yield directly the changes in the total molecular dipole moment produced by small distortions from the equilibrium configuration in the manner specified by Q_k. The fact that overtones appear with measurable intensity in the spectra of most molecules indicates that not all the assumptions underlying Equation (5) can be valid. Crawford and Dinsmore (17) have shown that mechanical and electrical anharmonicity in the potential function should have only minor effects on the intensities of fundamentals, but there is some doubt concerning the conditions under which the multipole moments corresponding to the higher terms in Equation (4) can be safely neglected (26).

The information given by Equation (5) is not very useful unless relations can be found which allow the magnitude and direction of the total moment change to be apportioned over the various stretching and bending motions of the chemical bonds in the molecule. If the molecule has symmetry, it is fairly easy to resolve the moment change parallel and perpendicular to the symmetry axis, but any detailed interpretation requires that the form of the distortion corresponding to Q_k be accurately known. This means that the potential energy of the molecule must be known under all possible distortions. Use of the measured frequencies in the secular equation is not sufficient for this purpose since there are, in general, fewer frequencies than there are force constants to be determined, so that additional data on the force constants must be sought through other methods. Once these have been determined, the matrix

methods developed by Wilson (81) may be used to extend the interpretation of the intensities.

The usual procedure is to choose a set of $3N - 6$ "symmetry coordinates", S_i, in terms of simple bond stretching and bending motions, so combined that each symmetry coordinate belongs to one of the symmetry species of the point group of the molecule. These may then be related to the normal coordinates by a linear transformation

$$Q_k = \sum_i (L^{-1})_{ki} S_i \qquad (6)$$

The evaluation of the coefficients $(L^{-1})_{ki}$ requires knowledge of the masses, force constants, and geometry of the molecule. The calculation has been carried out for the sulfur dioxide molecule in Appendix I of this thesis.

Since

$$\frac{\partial \vec{\mu}}{\partial S_i} = \sum_k \frac{\partial Q_k}{\partial S_i} \cdot \frac{\partial \vec{\mu}}{\partial Q_k} = \sum_k (L^{-1})_{ki} \cdot \frac{\partial \vec{\mu}}{\partial Q_k} \qquad (7)$$

the intensities are now related to the symmetry coordinates.

Further interpretation in terms of deformation of individual bonds requires further assumptions. Those most generally employed are:

(a) a change in length, dr, of a valence bond produces a moment change $\frac{\partial \mu}{\partial r} \cdot dr$ directed along the bond, $\frac{\partial \mu}{\partial r}$ being evaluated for the equilibrium configuration.

(b) a change, $d\theta$, in a bond angle θ produces a moment change $\mu_B \cdot d\theta$ perpendicular to the bond. Here μ_B is the "bond moment" in the equilibrium configuration, which in this

treatment should be identical with the "static bond dipole moment" derived from other methods.

(c) the bond moments are additive, their vector sum being the molecular dipole moment.

(d) the bond moments are independent, so that a moment change in one bond does not influence the moment in any other bond.

Such assumptions clearly refer to a molecular model in which each atom carries a fixed charge, and moment changes are considered to arise solely from the mechanical displacement of these charges as the molecule is distorted. The status of these assumptions will be discussed in connection with the results in Chapter V.

The sulfur dioxide molecule was chosen for study on several grounds. It is a non-linear triatomic molecule with an axis of symmetry, and consequently has three non-degenerate fundamental vibrations, two belonging to the totally symmetric species and one to the antisymmetric species. All three are infrared active, and lie within the frequency ranges accessible to the prisms which were available for use. At the time this work was undertaken, no results had been published on the infrared intensities, but excellent geometry and potential constants had been made available (53, 32, 43). The molecule was therefore attractive in terms of a study of bond moments, particularly with reference to reported differences in the moment derivatives obtained from vibrations of different symmetry (19, 50, 59, 60). The additional fact that its melting point (-72°C) and boiling point (-10°C) made all three phases accessible with relatively simple apparatus suggested its suitability for studies of intermolecular effects. Very similar arguments governed the choice of

carbon disulfide as a second molecule for study, together with the observation that the temperature range in which CS_2 is a liquid (-110°C to 46°C), is unusually great for a non-polar molecule of moderate molecular weight.

In the case of sulfur dioxide, the assumptions (a) to (d) above lead easily to simple relations permitting the calculation of the bond moments, and their derivatives with respect to the sulfur-oxygen interatomic distance. The symmetry coordinates are conveniently chosen to be

$$\begin{aligned} S_1 &= 2^{-1/2} (\Delta r_1 + \Delta r_2) \\ S_2 &= r \Delta\theta \\ S_3 &= 2^{-1/2} (\Delta r_1 - \Delta r_2) \end{aligned} \tag{8}$$

where r is the equilibrium S - O distance,

$\Delta\theta$ is the change in the O - S - O angle, and

Δr_1 and Δr_2 are the displacements of the oxygen atoms along the direction of the two S - O bonds.

These definitions lead to the following relations:

$$\frac{\partial \mu_{SO}}{r} = \frac{2^{-1/2}}{\cos \theta/2} \frac{\partial \mu}{\partial S_1} \tag{9}$$

$$\mu_{SO} = \frac{-r}{\sin \theta/2} \frac{\partial \mu}{\partial S_2} \tag{10}$$

$$\frac{\partial \mu_{SO}}{\partial r} = \frac{2^{-1/2}}{\sin \theta/2} \frac{\partial \mu}{\partial S_3} \tag{11}$$

2 The Influence of Finite Resolving Power on The Measurement of Infrared Intensities

The low dispersion of prism spectrographs and the low signal strengths obtainable with available combinations of sources and detectors in infrared spectrometers limit the spectral slit widths which may be employed to values of from 5 to 50 cm^{-1} in most wavelength regions. Rotational line widths at low pressures are generally much less than 1 cm^{-1}, and the total width of a vibration-rotation band is of the order of 100 cm^{-1} in most cases. The mechanical slit width, w, is generally wide enough that diffraction effects are negligible, and the distribution of transmission over frequencies on either side of the nominal frequency setting, ν_i, is approximately triangular (40). The spectral slit width, s, may be computed from the dispersion and geometry of the particular instrument for any value of w.

In consequence of this finite resolving power, the spectrometer does not record the true transmittance I/I_o at a frequency ν_i, but an apparent transmittance

$$\frac{T}{T_o} = \frac{\int S(\nu) \cdot e^{-k_\nu c l} \cdot f(\nu, s)\, d\nu}{\int S(\nu) \cdot f(\nu, s)\, d\nu} \qquad (12)$$

where $S(\nu)$ is the intensity distribution of the source,

$f(\nu, s)$ is the slit transmission function, and

the integration is over all frequencies accepted by the slit when the spectrometer is set at ν_i.

If the observed transmission curve of a sample is recorded and the apparent integrated absorption coefficient B is calculated according

to

$$B = \frac{1}{Cl} \int_{Band} ln \frac{T_o}{T} \, d\nu \qquad (13)$$

the quantity B will differ from A of equation (1) sometimes by a very large factor. It is necessary to choose conditions so that $S(\nu)$ and $e^{-k_\nu Cl}$ are both nearly constant over the spectral slit width if B is to approach A. This means that the spectral regions occupied by the absorption bands of atmospheric water vapor and CO_2 must be avoided unless these substances can be removed from the optical path, and that only very weak absorption bands will be closely followed by the spectrometer. Extensive discussion of these problems has been carried out, particularly by Neilsen, Thornton, and Dale (40), Ramsay (47), and most recently by Benedict, Herman, Moore, and Silverman (6), and Howard, Burch, and Williams (27).

In consequence of this effect of finite slit widths, the most generally accepted procedures for obtaining A involve an extrapolation to zero absorption, either by way of measurements on a series of diminishing cell lengths as in the method of Bourgin (10), or on a series of diminishing concentrations of the absorbing molecule as in the method of Wilson and Wells (71). When the band measured has rotational fine structure, k_ν is a rapidly varying function of ν within the spectral slit width, and the departures of T/T_o from I/I_o are large. The extrapolation curve is found to be steep and non-linear under these conditions. For this reason, it is a primary requirement of the extrapolation methods that sufficient pressure of a non-absorbing foreign gas be added to samples of absorbing gas in order to broaden the rotational lines until they merge into a

fairly smooth envelope. When this is done, a plot of $\int \ln \frac{T_o}{T} \, d\nu$ against the equivalent path length of the absorbing gas is a straight line through the origin in the region of low partial pressures, tending to slope off at higher partial pressures (see, for example, Callomon, McKean, and Thompson (14)). The limiting slope of this curve at the origin gives A, the true integrated absorption coefficient, independent of the spectral slit width. Alternatively, the intercept at zero path length of a plot of B versus path length will yield A directly. It is common to employ both plots in order to achieve the best smoothing of the experimental data, in view of the inherently large errors of measurement at very weak absorption.

While in principle an extrapolation to zero absorption is just as necessary in measuring bands in the liquid phase as in the gas phase, the absence of the rotational fine structure generally means that the apparent integrated absorption coefficient lies within 5% of the true value for spectral slit widths less than 0.65 of the bandwidth at half-maximum absorbance. This criterion and the extension of extrapolation methods to liquid phase measurements have been established by Ramsay (47).

3 Intensities of Infrared Bands in Condensed Phases

In high pressure gases or condensed phases the collision frequency becomes comparable to or greater than the rotational frequencies, so that it is doubtful whether any significance attaches to the idea of quantized rotational states. It is observed that the rotational branches of vibration-rotation bands disappear, being replaced by an envelope which approximates to a Lorentz curve around a central frequency which is

displaced from the central frequency in the gas phase by a few percent (47). Intensity changes are known to occur (21, 66) but little quantitative information is available (44) except on intensities in various solvents (22, 4, 29, 33).

The only theoretical discussions of intensities in the liquid phase appear to be those based on the theory of dielectric polarization as developed by Lorentz (78), Debye (74), Onsager (41), and others (13, 73). It is assumed that, whatever other specific interactions may occur between a molecule and its neighbors, any electric moment in the molecule will impose a field on neighboring molecules which will polarize them, and the resulting induced moments will impose a reaction field on the original molecule which will serve to modify its internal fields. Kirkwood, Bauer, and Magat (5) have given an expression for the frequency shifts to be expected on this model, which has been considered to provide a reasonable base-line such that shifts greater than those predicted are taken to indicate specific interactions, such as hydrogen bonding (22, 29, 67). Chako (15) has given the following relation for the ratio of the intensity A_ℓ of an absorption band of the solute in a dilute solution to the intensity A_g of the same band in the gas phase,

$$\frac{A_\ell}{A_g} = \frac{1}{n}\left[\frac{n^2 + 2}{3}\right]^2 \qquad (14)$$

where n is the refractive index of the solvent at the frequency of the absorption band, and the relation is intended to hold for dilute solutions only. More recently, Polo and Wilson (44) have given a relation of identical form in which A_ℓ is now the intensity in the pure liquid of a band whose gas phase intensity is A_g, and n is the refractive index of

the liquid. The expression is shown to result from either the Debye or the Onsager models of dielectric polarization, and is stated in their paper to be not strictly applicable to solutions, and to be the same irrespective of whether or not the molecule has a permanent dipole moment. There appears to be some discrepancy between these two presentations. It is not easy to see how the Polo and Wilson relation is to be applied, since the condition $\mathcal{E} = n^2$ requires that both $\mathcal{E}$ and n be defined at the same frequency, and n is a rapidly varying function of frequency in the region of an absorption band.

The assumptions which underlie the several formulations of the theory of dielectric polarization have been discussed by Brown (73), and they are such as to offer little hope that the detailed influence of neighboring molecules on the electric charge distribution in an absorbing molecule will be well described in terms of what are essentially macroscopic concepts.

The very great influences of adjacent molecular structure on the infrared intensities associated with various structural groups in molecules which have been reported (4, 26, 72) emphasize the sensitivity of the infrared intensity to the details of the molecular charge distribution. This suggests that the effects of the much weaker intermolecular forces may still be observably great, and that they will yield useful information on these forces, particularly where the interactions are strongly dependent on the mutual orientations.

Since in the present work variation of temperature has been used as the means of varying the intermolecular interaction, two comments

are in order on the influence of temperature on infrared absorption bands in liquids. The first is that, in the absence of intermolecular interactions other than collisions, the bandwidth would be expected to vary with temperature while the integrated area (transition probability) remained unaltered. If the bandwidth is taken to be proportional to collision frequency, it should vary as the square root of the absolute temperature. Assuming a Lorentz contour for the band, its peak height should be inversely proportional to the temperature. Departures from this pattern of behavior should be indicative of departures from the "rigid non-interacting spheres" model of the liquid state, and should thus be measures of intermolecular interaction. The second comment is that although the observed intensity in the frequency region of a fundamental may contain significant contributions from "hot-bands" (absorption transitions in which the lower state is not the ground state) variation of temperature should not influence the integrated band area since decreased hot-band contributions at lower temperatures would be exactly compensated by increased fundamental absorption, provided that all transitions involved have equal probabilities. While the latter condition may not be accurately fulfilled in all cases, departures from it imply a degree of charge redistribution which is quite unlikely in the low-energy vibrational states of most molecules. It should be noted, however, that where the hot-band and fundamental frequencies differ slightly, the band shape should vary with temperature.

CHAPTER III

EXPERIMENTAL PROCEDURES

The majority of spectra were recorded using a Perkin Elmer Model 21 Spectrophotometer. In this instrument radiation from a Nernst glower is passed in a double-beam arrangement through sample and reference cells, and is chopped at 13 cycles per second so that in alternate half-cycles radiation passing each cell falls on the entrance slit of a prism spectrometer. The thermocouple detector is connected through a narrow band amplifier, synchronous detector, and 60 cycle servo system to a linear wedge aperture which moves across the reference beam to match its intensity with that of the sample beam. A pen, mechanically coupled to the intensity wedge, records optical density on a suitable semilogarithmic paper while the spectrometer scans linearly in wavenumber by means of a motor-driven cam system. Rocksalt and potassium bromide prisms were used in the appropriate frequency regions.

1 Vapor Samples of Sulfur Dioxide

(a) Gas Handling Procedure

The absorption cells used for gaseous samples were 10.0 cm in length and were fitted with windows of rocksalt, potassium bromide, or silver chloride as required. Cell bodies of glass were used for most of the work, since metal cells showed adsorption effects.

The vacuum system used for filling the absorption cells is

shown in Figure 1. Pressures greater than 40 mm Hg were read from an open-end mercury manometer to an accuracy of ± 0.5 mm or better. Pressures less than 40 mm Hg were read from a differential oil manometer. The density of the gauge fluid was determined gravimetrically to be 1.050 gm/cc at 20°C. Readings from this gauge should be accurate to ± 0.05 mm Hg.

The sulfur dioxide used was obtained from the Matheson Chemical Company, the advertised purity being 99.7%. It was found to contain a few percent of a gas not condensable at the temperature of liquid oxygen, and the liquid condensed directly from the cylinder had a pronounced yellow color. The sulfur dioxide was therefore purified by one or more vacuum distillations. The vapor from a sample which had undergone a single distillation was subjected to mass spectrometric analysis which showed a purity greater than 99%.

The sulfur dioxide was frozen out under vacuum with liquid oxygen. The absorption cells were pumped out and were tested for leakage and desorption of vapors before each filling, by means of the differential manometer. The desired pressure of vapor was obtained by opening the stopcock A, checking that there was no detectable rise in pressure, then slowly warming the liquid until the desired manometer readings were approximated. Stopcock A was then closed, and the manometer was checked until steady readings for several minutes indicated that temperature and adsorption equilibria obtained. The cell stopcock was then closed, and the remainder of the system re-evacuated. With stopcocks A and B closed, dried nitrogen gas was admitted at C in a moderate stream. When the nitrogen pressure exceeded the pressure of vapor in the cell by several

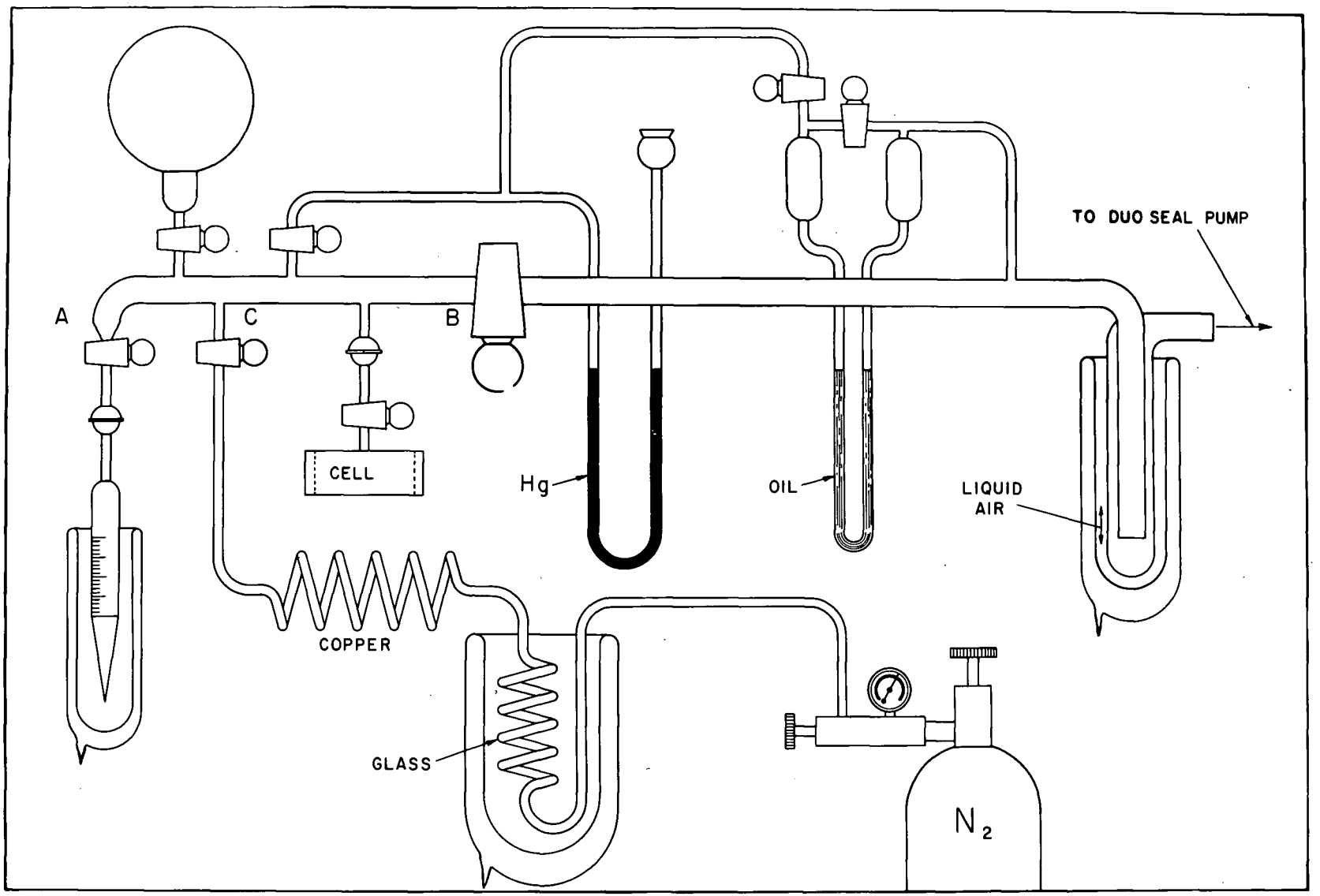

Figure 1. Gas handling apparatus.

centimeters of mercury, the cell stopcock was opened and the pressure was allowed to rise steadily, the cell stopcock being closed as the desired total pressure was reached. In this way no opportunity for loss of vapor from the cell was permitted, at the expense of about 10 mm accuracy in the nitrogen pressure determination.

The need for drying the premium-grade nitrogen was demonstrated in the course of attempts to use a Perkin Elmer one-meter path length absorption cell in order to extend the intensity measurements to lower partial pressures. The band intensities were found to decrease rapidly with time after cell filling. The rate of decrease was greatly reduced when the nitrogen was dried by passage through a glass helix in liquid oxygen. A long copper helix at room temperature was used to avoid large temperature error in the added nitrogen. The sample temperature was taken to be the room temperature which was close to 25°C for all runs.

(b) Effects of Adsorption and Incomplete Mixing

Tests in which the spectrum of a sample was recorded at several times from ten minutes to more than six hours after filling showed that the SO_2 concentration remained constant with time in glass-bodied cells, while some cells having brass or cast aluminum bodies showed serious and prolonged adsorption effects. Results obtained with cells showing adsorption were discarded.

Incomplete mixing of the absorbing gas with the broadening gas has been found by Penner and Weber (42) to be an important source of error in high pressure studies. In a number of tests in which Teflon chips were placed in the cell, and the spectrum was recorded before and after

vigorous agitation, no suggestion of incomplete mixing was ever indicated. The tests were conducted at total pressures of one and three atmospheres.

(c) The Accuracy of the Partial Pressures

The accuracy of the manometric pressure determinations was confirmed by quantitative chemical analysis of the contents of the absorption cell after the spectrum had been run. Gas from the absorption cell was drawn slowly, at reduced pressure, through two glass traps, in series, cooled by liquid oxygen, until several cell volumes of gas had been flushed through the cell and there was no residual absorption by ν_3. While cold the traps were charged with 15 ml of ammoniacal hydrogen peroxide. They were then warmed slowly to room temperature with constant agitation. These solutions were then analyzed for sulfur as $BaSO_4$ by standard gravimetric procedure (80). The results are given in Table I.

TABLE I

Comparison of Partial Pressures of Sulfur Dioxide Determined from Gauge Readings and from Gravimetric Analysis of $BaSO_4$

	Pressure of SO_2 mm Hg			
by Gauge	8.29	12.4	20.4	20.7
by $BaSO_4$	8.56	12.96	18.9	19.7
% Difference	-3.2	-4.3	+7.9	+5.0

The efficiency of the traps is indicated by the fact that 97.5% and 98.2% of the SO_2 was found in the first trap for the 12.4 and 20.4 mm

samples respectively. It may be concluded that the partial pressures read from the oil manometer are free of systematic error to within about 2%, though the scatter of the analytical results does not permit any given pressure to be assigned within better than 5%.

(d) Determination of Integrated Absorption

The samples were run with a scanning speed of about 10 minutes per 100 wavenumbers, which permitted a high degree of filtering against random noise with sufficient gain to keep the pen response much faster than the rate of change of intensity. The noise in the trace was less than 1/4% transmission.

The areas under the absorption curves were calculated by Simpson's Rule, using an interval small with respect to the half-intensity width of the bands. The sums of the odd and even ordinates generally agreed to better than 0.1%, and in no case did they disagree by more than 2%, from which it may be concluded that the integration procedure is not significantly in error. Moreover, this procedure should give an estimate of the area which is biased in the same sense as the recorded area is biased by the effect of the finite resolution of the spectrometer. The error from both sources should vanish in the extrapolation to zero absorption.

Background corrections were applied from the recorded spectrum of the absorption cell filled with dry nitrogen. A reference cell of the same length and window materials, filled with dry nitrogen, was used in the reference beam so that the background corrections for ν_3 and ν_1 were very small. The frequency range of ν_2 extended beyond the optimum

working limit of the KBr optics so that higher noise, sluggish response, and greater background were met with in the low frequency tail of the band. This was met by integrating in the region of high instrument performance and estimating the contribution of the low frequency tail (approximately 7%) by symmetry from the high frequency tail.

Corrections for stray radiation were made wherever the stray radiation was found to exceed 1%, though the error from this source should also vanish because of the extrapolation procedure.

The reproducibility of the instrument in runs on the same sample, or in runs on cells filled to the same partial pressure was better than 2%, usually about 0.5%.

The overall accuracy of the measured band areas varies with the band measured, but no grounds were found for believing that they could be in error by more than 5%.

2 Liquid and Solid Samples

For studies at room temperature, the sealed liquid absorption cells were of conventional design with amalgamated lead spacers. For work at low temperatures, a spring-loaded cell assembly was designed to ensure that the cell thickness would be that of the spacer at all temperatures, and to maintain constant stress on the cell windows.

A major difficulty in the design of absorption cells for infrared work is the scarcity of materials having good mechanical properties and chemical resistance in combination with optical transmission over the desired frequency ranges. For work with sulfur dioxide the alkali

halides, especially KBr, have poor chemical resistance. Materials such as periclase and arsenic trisulfide transmit only ν_3 of SO_2 well, and ν_2 not at all. Thus, silver chloride is the window material of choice, but its mechanical properties served to defeat all attempts to construct and preserve a uniform cell having a known thickness of between one and three microns. These thicknesses were found to be necessary for intensity measurements on liquid SO_2 bands in spite of the reported data of Maybury, Gordon, and Katz (35). One cell constructed had an apparent thickness of 1.3 microns when calibrated using ν_3 of CS_2, but was later shown to be non-uniform to a serious extent. A uniform cell having a cellophane spacer 16.6 μ thick by interference fringes was the best compromise obtained in the available time. Since this work was completed, Adams and Katz (1) have published results on a variable-space silver chloride cell which can be used at 5 microns thickness. Their success was made possible by the choice of a small aperture to reduce the effects of plastic flow of the windows, a choice forbidden to us by the geometry of the cooling arrangements.

For very intense absorption in the frequency region 4000 to 1200 cm^{-1} by substances liquid at room temperature, a special cell was constructed which is illustrated in Figure 2. It is essentially a small Fabry-Perot interferometer, having periclase windows selected for optical flatness to $\pm$ 0.1 microns, one of which is channelled at the edges of the region traversed by the light beam. These features were found to be essential in the construction of cells thinner than about 5 microns. Such thin cells require very flat windows if their uniformity is to fall within limits which will permit accurate intensity measurements; the required

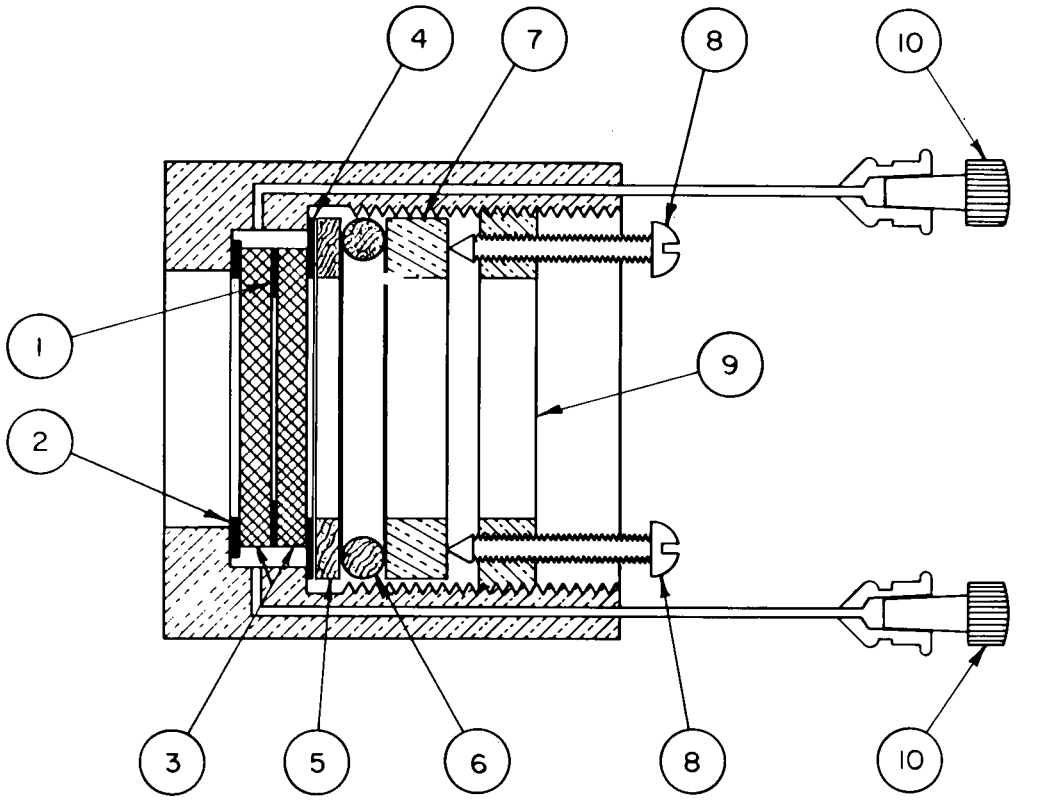

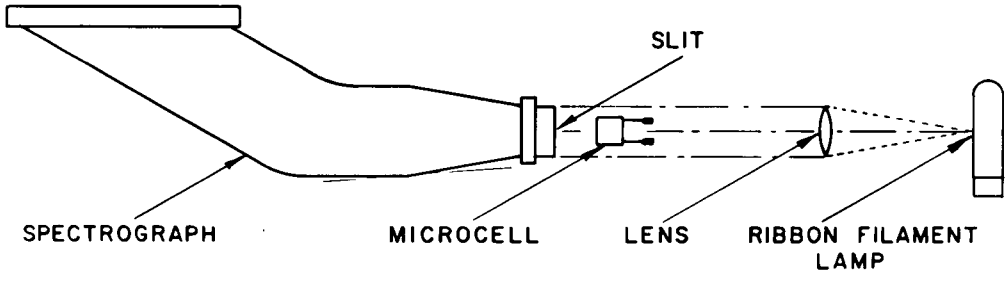

1	EVAPORATED GOLD.	6	"O" RING
2	Pb AMALGAM.	7	PRESSURE RING
3	MgO PERICLASE OPTICAL FLATS	8	LEVELLING SCREW
4	POLYETHYLENE	9	RETAINING RING
5	RUBBER RING	10	TEFLON PLUGS

Fig - 2 Microcell and arrangement for thickness calibration

limits were computed by integrating Lambert's law over various non-uniform cell-thickness profiles. The channelling is needed to ensure that the region of the cell first filled by the capillary film is the portion in the beam, so that air bubbles are not trapped in this zone. The spacers used were films of gold, evaporated onto the windows. The exclusion of tiny dust particles from between the plates presented a major problem in assembly, which was met with fair success by removal of individual particles under a microscope, then holding the two clean surfaces together by means of the surface tension of a film of a very clean volatile solvent during assembly. The diameter of the periclase optical flats available was only 16 mm, so that the cell had to be mounted at the first focus of the source system inside the spectrometer housing, a condition which demanded thorough sealing of the cell and prevented cooling of the cell below room temperature. The assembled cell was adjusted to parallelism by examining the Edser-Butler fringes in a medium quartz spectrograph with the cell in front of the slit, as shown in Figure 2, and use of the levelling screws. The pattern of parallel fringes obtained was photographed for selected areas of the cell, and the thickness and uniformity of the cell were computed from the photographs. The gaskets required for sealing caused the thickness to be slightly unstable with time and sensitive to rough handling. Results were accepted from this cell only when the fringe patterns before and after absorption measurements established that no changes had occurred.

The microcell just described was used at thicknesses of 2.59 and 2.44 microns ($\hat{\sigma} = \pm 0.11$ from 10 observations), to determine the integrated absorption coefficient for the ν_3 band of liquid CS_2, given

in the following chapter, and for some other bands in water, D_2O, and methanol which will not be reported on the grounds that they have little relation to the rest of the work discussed, and were not very extensive. Still thinner cells were needed, since the peak optical densities often exceeded 1.0, but the fringe patterns for thinner cells are too diffuse for accurate thickness determinations. Where high peak absorption was met, a neutral filter of wire mesh having an optical density of 0.68 was used in the reference beam to bring the peak absorption to a level where the intensity wedge has better accuracy. Slit width and amplifier gain were selected to make use of the filter possible, if required, without loss of response.

Cooling of cells below room temperature was done using a simple cold box similar to that described by Bernstein (8). It consisted of a Lucite box, insulated with Styrofoam, having double windows for the entrance and exit of the beam. The space between the windows was continuously evacuated and heating coils were wrapped on the mountings of the outer windows to avoid condensation. Cooling was done by rapidly flowing air (1 to 5 ℓ/min), which was dried in a series of large diameter traps and cooled by passage through a copper helix in liquid oxygen before entering the box. Temperatures could be maintained down to -90°C. The cooling air served to remove any vapor of the sample from the optical path. In order to compensate for reflection and absorption losses and for defocussing of the beam, a similar uncooled box was placed in the reference beam. This box was swept with dried air to equalize atmospheric absorptions in the two beams. The great thickness of window material made the angular position of the windows in the beams quite

critical in maintaining the alignment of the beams.

Samples of liquid sulfur dioxide were purified as outlined in Section 1 (a) of this chapter. Carbon disulfide was purified by two fractional distillations through a three-foot glass-packed vacuum-jacketed column at atmospheric pressure with a reflux ratio of 10 to 1, at a rate of 100 cc/hr, the mid-50% of each pass being retained. It was stored in the dark, being subject to slow photochemical discoloration.

CHAPTER IV

RESULTS

1 Gas Phase Intensities for SO_2

Table II gives the partial pressures of sulfur dioxide and the corresponding band areas observed with a 10.0 cm path and with dry nitrogen added to a total pressure of 760 mm. The integrated absorption coefficients A_i (see p. 4), were obtained from these data in two ways.

The slope at the origin of a plot of band area against partial pressure was obtained by drawing a line of best fit through the points by visual estimation. The lines were sufficiently close to linear in the region of low partial pressures to permit the tangent at the origin to be drawn with confidence. The experimental points and the tangent lines drawn from them are shown as Figures 3, 4, and 5, for ν_1, ν_2, and ν_3 respectively. The relation of the experimental points to these tangent lines indicates that while small departures from complete pressure broadening were observed at the higher partial pressures, the broadening at lower pressures was essentially complete (14). This conclusion is supported by the measurements shown in Table III, which show the effect of increasing the total pressure on the band areas observed with a fixed partial pressure of sulfur dioxide in a 3.94 cm glass-walled absorption cell. The error due to incomplete pressure broadening at a total pressure of one atmosphere is certainly less than 2% for the partial pressures used here.

TABLE II

Partial Pressures, Band Areas, and Apparent Integrated Absorption Coefficients for the Fundamentals of Sulfur Dioxide

ν_1			ν_2			ν_3		
p	Area	B	p	Area	B	p	Area	B
60.5	32.6	2.11	62.8	35.8	2.24	14.7	56.7	1.51
23.8	12.4	2.04	29.1	17.9	2.41	12.4	46.3	1.46
20.7	11.55	2.14	28.4	17.2	2.38	12.12	45.9	1.49
20.4	11.25	2.16	21.4	14.03	2.57	9.61	36.1	1.47
14.7	7.79	2.08	16.9	10.7	2.48	8.29	32.4	1.53
12.40	6.67	2.11	13.4	8.57	2.42	6.75	27.5	1.60
12.12	6.72	2.17	10.2	6.63	2.55	5.10	20.8	1.60
9.61	5.00	2.04	7.03	5.11	2.85	4.88	20.9	1.68
8.29	4.42	2.09	4.82	2.89	2.35	4.88	20.8	1.67
6.75	3.84	2.24				4.37	17.9	1.61
6.60	3.61	2.14				4.32	17.5	1.59
5.01	2.70	2.12				3.49	15.0	1.69
4.37	2.48	2.22				2.62	11.37	1.70
4.32	2.44	2.22				2.07	9.29	1.76
3.49	1.88	2.12				1.60	7.23	1.77
1.60	0.85	2.08				0.88	3.83	1.71

Units of p are mm Hg.

Units of Area are $(cm^{-1}/2.303)$.

Units of B are 10^3 litres $moles^{-1}$ cm^{-2} at 25°C.

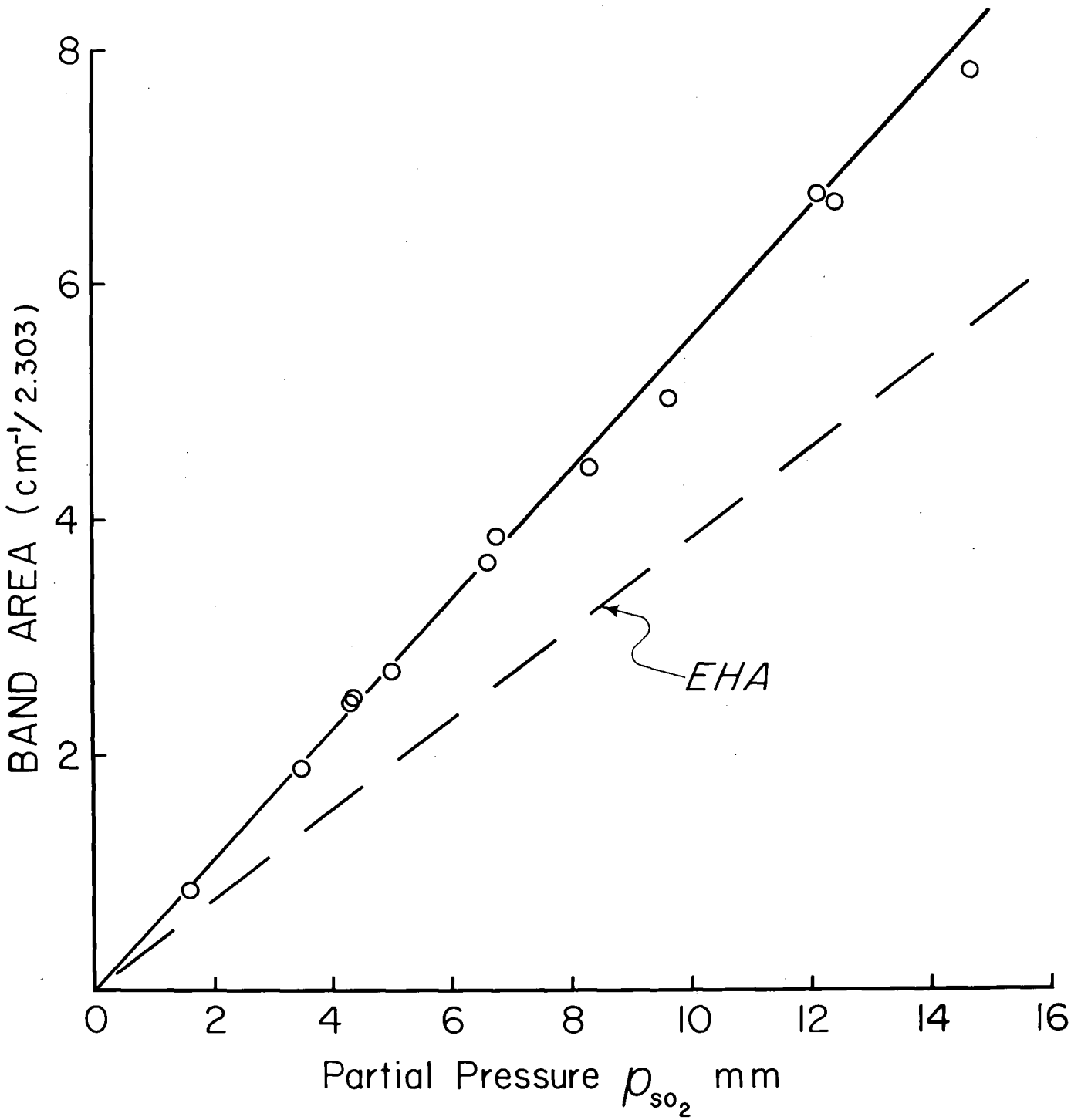

Figure 3. Limiting-slope extrapolation for ν_1 of sulfur dioxide. The slope of the dashed line corresponds to the intensity reported by Eggers, Hisatsune, and Van Alten.

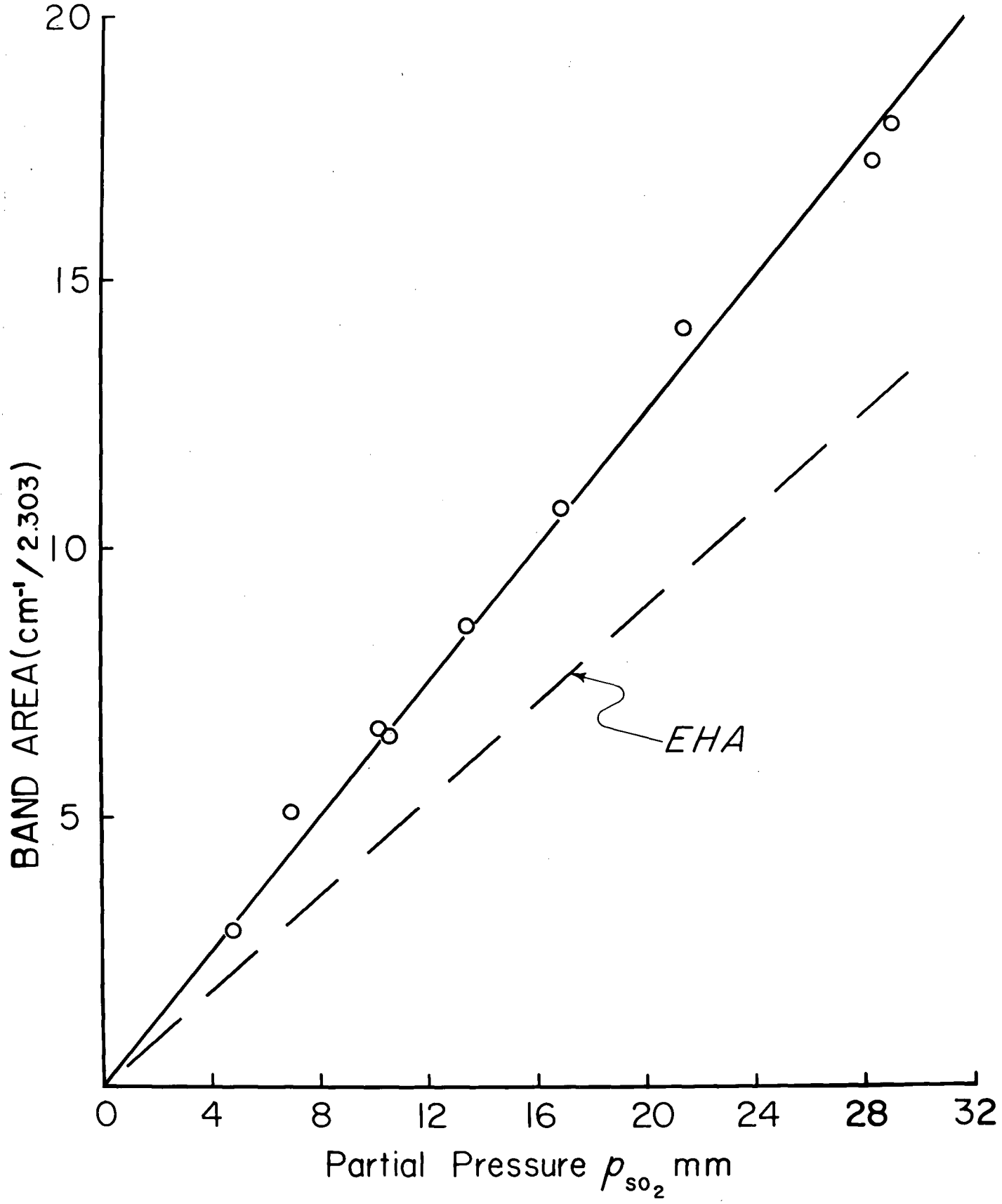

Figure 4. Limiting-slope extrapolation for ν_2 of sulfur dioxide. The slope of the dashed line corresponds to the intensity reported by Eggers, Hisatsune, and Van Alten.

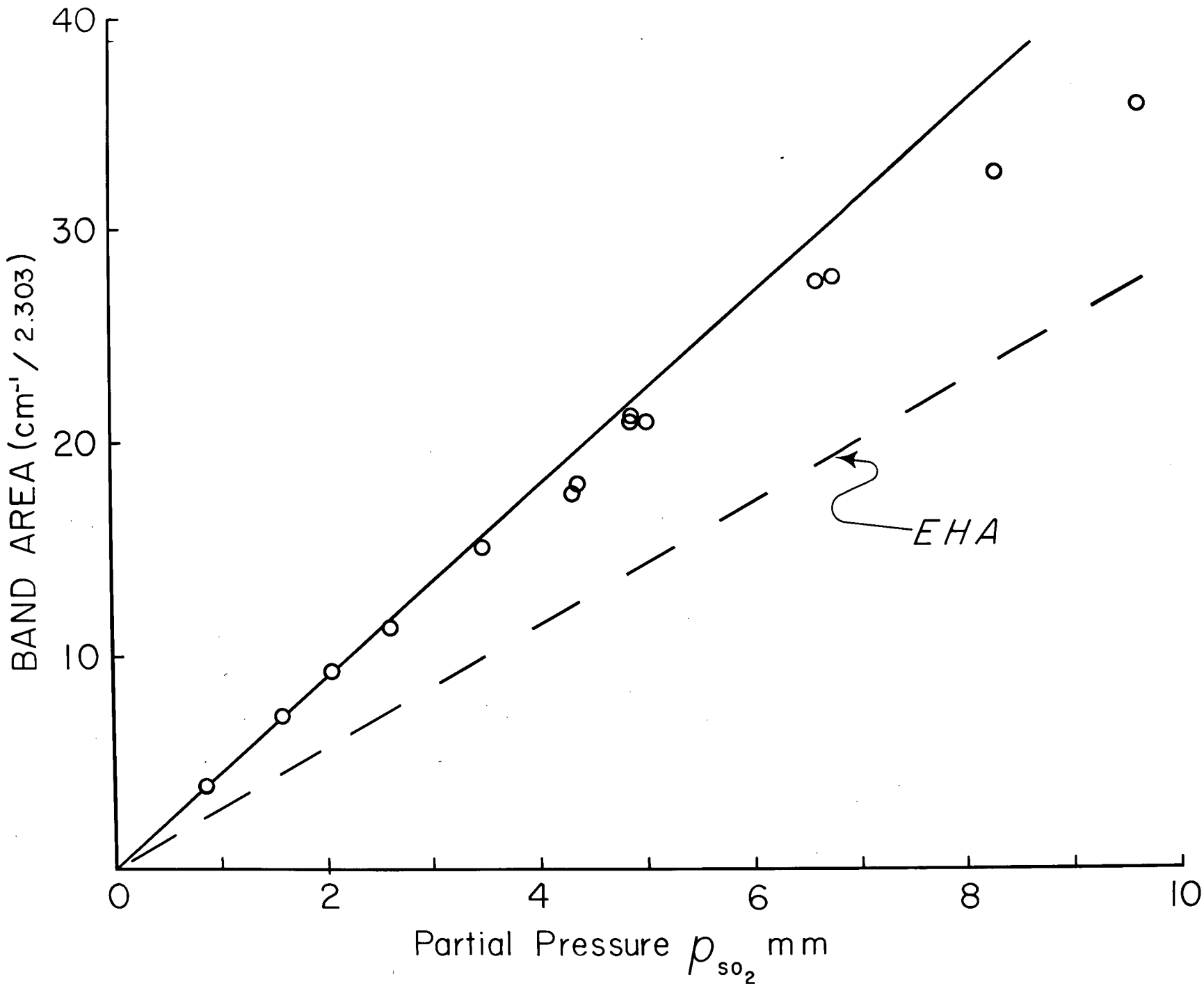

Figure 5. Limiting-slope extrapolation for ν_3 of sulfur dioxide. The slope of the dashed line corresponds to the intensity reported by Eggers, Hisatsune and Van Alten.

TABLE III

Variation of Band Area with Total Pressure
at Constant Partial Pressure of Sulfur Dioxide

p	ν_3			ν_1		
	P = 293	P = 760	P = 2300	P = 293	P = 760	P = 2300
16.07	22.77	23.34	23.34	3.49	3.52	3.54
9.85		15.15	15.02			
5.37		8.36	8.36			

Units of p and P are mm Hg.

Units of band area are ($cm^{-1}/2.303$).

The " limiting slope extrapolation" just described has the disadvantage of giving too great weight to the points near the origin where the experimental accuracy is lowest. An alternative procedure is to calculate the apparent integrated absorption coefficient, B', (see p. 11), and plot B' against the partial pressure. This procedure gives a clearer indication of the overall accuracy of the measurements, but tends to place too much emphasis on the trend of points at higher partial pressures. In consequence of this, the values of the true integrated absorption adopted on the basis of these measurements were obtained in the following way. Values of B' were calculated for various points lying on the best-fit lines of the limiting slope extrapolation curves, and used to determine the form of the curves to be expected in the plots of B' versus p, Figure 6. The best-fit lines were then redrawn on both plots, and the procedure repeated until both extrapolations gave the same values for the A_i, and optimum fitting of the experimental points. This smoothing procedure should distribute the weight reasonably well over all points. The above procedures were adopted where it was shown that least-squares fitting of polynomials did not provide a reasonable, consistent pattern for treating all three fundamentals. In the least-squares procedure, the weight attached to the points at higher partial pressures makes the limiting slope at the origin quite sensitive to the number and order of the higher terms included in the polynomial. These difficulties can be avoided where sufficiently high broadening pressures can be used, but are replaced by difficulties of technique (42, 63, 21), which led to the choice of conditions used in these measurements.

The integrated absorption coefficients obtained, corrected to

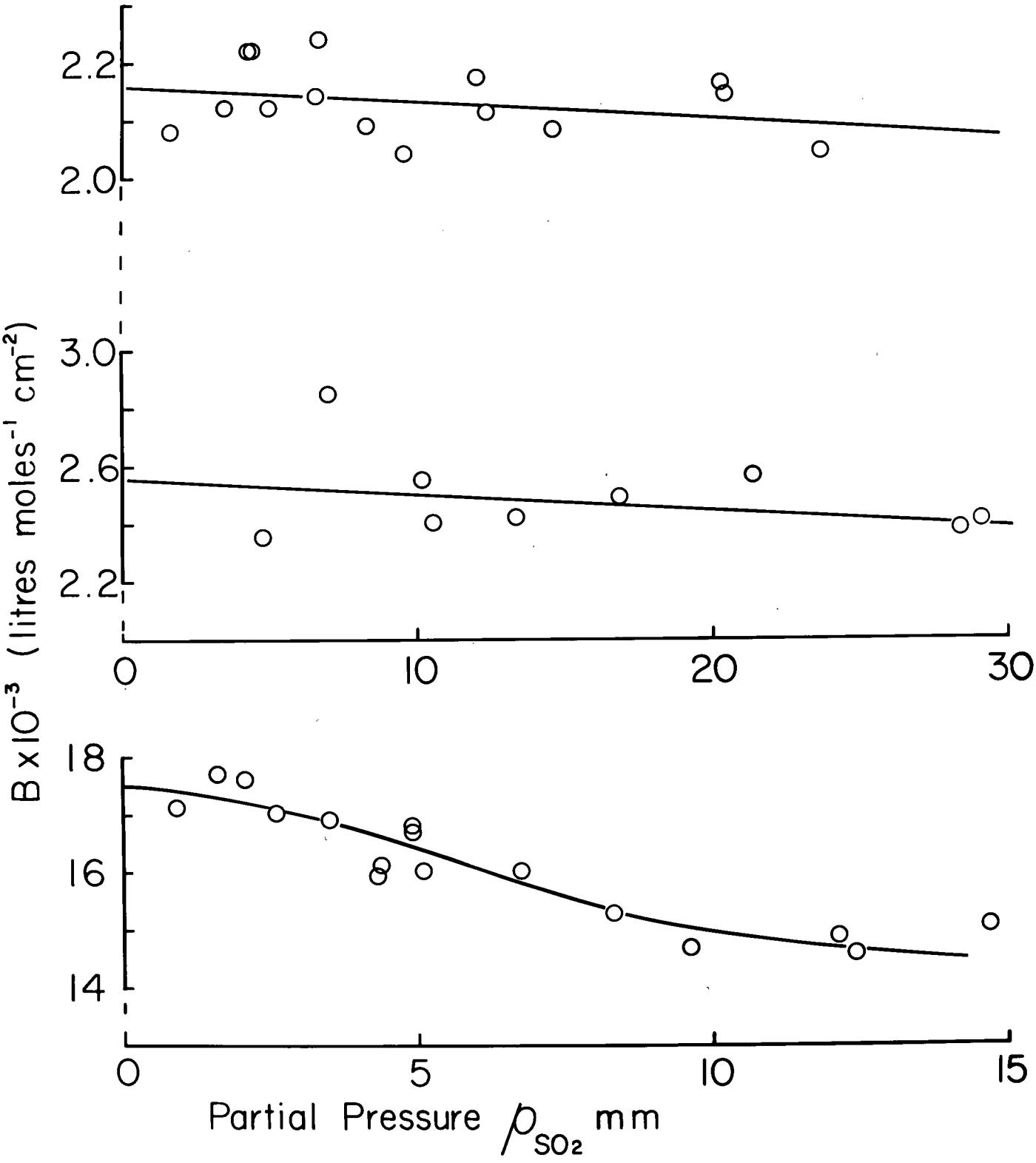

Figure 6. Apparent integrated absorption coefficients of the sulfur dioxide fundamentals as a function of partial pressure, at 25°C and a total pressure of 760 mm.

standard temperature and pressure, are presented in Table IV, together with an estimate, based on the scatter of the plots of B versus p, of the limits of uncertainty in their determination from the present data.

During the time that this work was in progress, a paper was published by Eggers, Hisatsune, and Van Alten (19) containing the results of measurements on the band intensities of sulfur dioxide. Their results, which are included in Table IV and are indicated on Figures 3, 4, and 5 by dashed lines, differ from those reported here by a factor considerably in excess of the estimated error in either investigation. This disagreement is discussed at the beginning of the next chapter.

The derivatives of the total molecular dipole moment with respect to the symmetry coordinates ($\partial\mu/\partial S_i$), were calculated as outlined in Chapter II and Appendix I, and are presented in Table V together with the corresponding values given by Eggers, Hisatsune, and Van Alten (19).

The assumptions concerning the additivity of bond moments and Equations 9, 10, and 11 which follow from them were applied to give values for the dipole moments of the S - O bonds in sulfur dioxide and for their derivatives with respect to the interatomic distance. These results are included in Table V.

2 Liquid and Solid Phase Studies

Attempts to obtain the spectrum of liquid and solid sulfur dioxide in films of sufficient thinness and uniformity to permit quantitative intensity measurements met with a very limited degree of success. In spite of this, the results are of some interest and are

TABLE IV

Comparison of Integrated Absorption Coefficients and Moment Derivatives for SO_2 from EHA* and from This Work

	Band	A x 10^{-10} sec^{-1} cm^{-1} at S.T.P.		$\partial\mu/\partial Q_k$ x 10^{10} esu	
	cm^{-1}	EHA	This Work	EHA	This Work
ν_1	1151	226	317 ± 8	± 49.1	± 58.1
ν_2	519	257	376 ± 20	± 52.3	± 63.6
ν_3	1361	1606	2560 ± 70	± 130.8	± 165.2

* EHA refers to Eggers, Hisatsune and Van Alten, J. Phys. Chem. 59, 1124 (1955).

TABLE V

Moments Calculated for Sulfur Dioxide

Moment	Relative Signs of $\partial\mu/\partial Q_1$ and $\partial\mu/\partial Q_2$	EHA	This Work
$\partial\mu/\partial S_1$	same	± 3.04	± 3.62
	different	± 1.443	± 1.69
$\partial\mu/\partial S_2$	same	± 1.45	± 1.80
	different	∓ 1.53	∓ 1.88
$\partial\mu/\partial S_3$	----	± 5.11	± 6.44
$\partial\mu_{SO}/\partial r$ (from ν_1 and ν_2)	same	± 4.27	± 5.09
	different	± 2.03	± 2.38
μ_{SO} (from ν_1 and ν_2)	same	∓ 2.46	∓ 2.98
	different	± 2.56	± 3.12
$\partial\mu_{SO}/\partial r$ (from ν_3)	----	± 4.17	± 5.27

Note: 1. Values of μ_{SO} are in Debyes; all others are esu x 10^{10}.

2. EHA refers to Eggers, Hisatsune, and Van Alten, J. Phys. Chem. 59, 1124 (1955). The values shown are not those of the original paper but have been recalculated from their intensity values, after correction of two of the formulae of their paper.

presented here together with observations on the spectrum of carbon disulfide in the pure liquid phase and in solutions in organic solvents. The band parameters which may be studied in investigations of this type are the frequencies of maximum absorption, the shapes of bands, the widths of the bands, and their integrated absorption coefficients.

(a) Frequencies and Shapes

The frequencies of maximum absorption observed for the samples studied in this work are presented in Table VI, together with corresponding observations by other workers. Sample spectra are reproduced in Figure 7. In the gas phase the centres of the parallel bands ν_1 and ν_2 are readily identified, while the origin of the perpendicular band ν_3 must be obtained from the analysis of high resolution data and is thus not specified in this work. In the pure liquid phase, the present measurements pertain to temperatures below -50°C, while those of Maybury, Gordon, and Katz (35) were made at room temperature. The agreement is probably within the combined errors of calibration for ν_1 and ν_2, but our estimate of the centre of gravity of the ν_3 band lies about 5 cm^{-1} below the figure of 1338 cm^{-1} given by them.

The frequencies recorded in this work for frozen SO_2 at -80°C differ considerably from those listed by Wiener and Nixon (69) for SO_2 at -180°C. Moreover the band shapes differ extensively between these two studies, a fact which may indicate a difference in the crystalline form of the samples studied. It appears possible to choose the frequencies from their published curves in a different manner from those listed by them, but not in such a way as to remove the disagreement between the two

TABLE VI

Frequencies of SO_2 Bands in cm^{-1}

Band	Gas		Liquid		Solution 10% in $CHCl_3$	Solid	
	This Work	SNF	This Work	MGK	This Work	This Work	WN
ν_1	1151	1151.38	1145	1148	1145	1145	1147 1142
ν_2	520	517.69	524	523	---	540 523	532 521
ν_3	---	1361.76	1355 1330 1315	1338	1338	1350 1336 1310	1330 1316 1308

SNF refers to Shelton, Nielsen, and Fletcher, J. Chem. Phys. 21, 2178 (1953).

MGK refers to Maybury, Gordon, and Katz, J. Chem. Phys. 23, 1277 (1955).

WN refers to Wiener and Nixon, J. Chem. Phys. 25, 175 (1956).

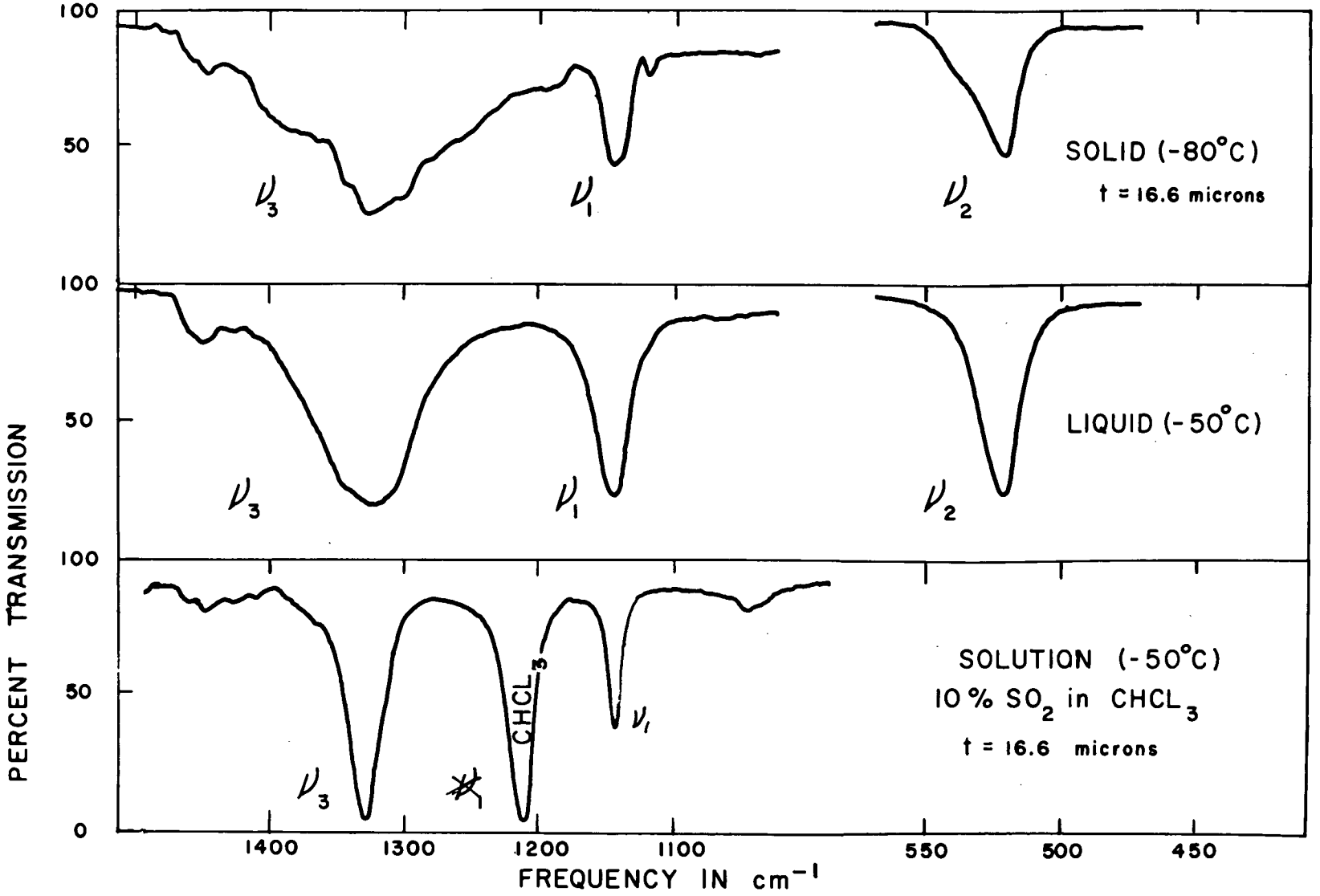

Figure 7. Spectrum of sulfur dioxide in condensed phases.

sets of data. It is possible for reflection phenomena in the polycrystalline films studied to distort the band contour recorded, but in both their work and ours the absence of strong scattering at frequencies far from the band centres was taken as indicating that the contours recorded corresponded to the true absorption envelope. The spacings of the various components in this study do not fit the interpretation of Wiener and Nixon in terms of combinations of ν_1 and ν_3 with lattice frequencies.

When a 10% solution of SO_2 in $CHCl_3$ was examined, the frequency found for ν_1 was the same as in pure liquid SO_2. For ν_3, on the other hand, the frequency in the solution appeared to be about 5 cm^{-1} higher than the estimated band centre for the pure liquid, while the triplet structure found in the pure liquid was absent in the solution.

Very similar observations resulted from measurements on some bands of carbon disulfide in the pure liquid, and in solution in chloroform or carbon tetrachloride. Observations were made at room temperature, and at temperatures down to -50°C, on the asymmetric stretching frequency ν_3 and on the combination band ($\nu_3 + \nu_1$) of the asymmetric and symmetric stretching frequencies. Sample spectra are given in Figure 8, and the frequencies recorded are presented in Table VII.

The multicomponent structure found for ν_3 in the pure liquid showed no temperature coefficient in the range investigated. On dilution of the CS_2 with chloroform or carbon tetrachloride, the structure changed progressively with the concentration in the manner indicated by Figure 8, and Table VII. It should be emphasized that the cell thickness was chosen for each strength of solution in order to keep the peak heights and

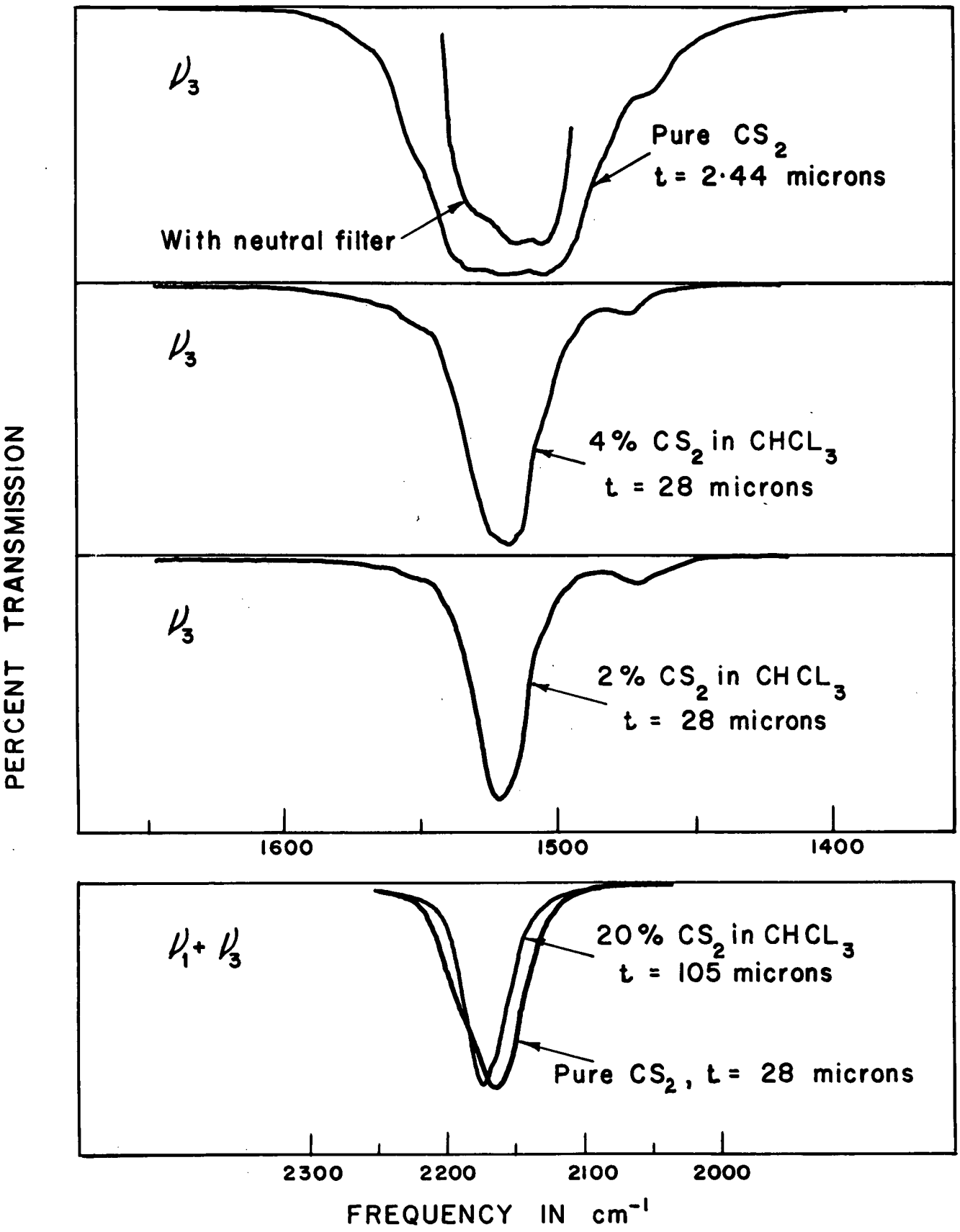

Figure 8. Absorption bands of carbon disulfide in the pure liquid and in solution.

TABLE VII

Frequencies of CS_2 Bands in $CHCl_3$ Solutions

% CS_2	100	50	20	4	0.4
ν_3 region	1570 ± 5	1570			
	1555 ± 5	1555	1555?		
	1530 ± 5	1535	1535	1535?	
			1520	1520	1521
	1516 ± 3	1516	1515	1515	1515
	1505 ± 3	1505	1505	1505	1505
	1495 ± 5	1495	1500	1500	
	1470 ± 5	1470	1470	1470	
$(\nu_3 + \nu_1)$ region	2190 ± 5		2190?		
			2173		
	2163 ± 2		2163?		
	2150 ± 5		2150?		

Notes: 1. Frequencies of maximum absorption are underlined.

2. The error values given with the frequencies for pure CS_2 are the uncertainties in locating the peaks or shoulders rather than errors of calibration.

3. The frequencies quoted for pure CS_2 and for the 20% solution were measured at 25°C and -50°C. The other solutions were studied at 25°C only.

4. Solutions in CCl_4 gave contours for ν_3 which were indistinguishable from those observed for chloroform solutions of the same mole fraction.

band areas roughly constant, so that the disappearance of components from the structure is due to real changes in relative intensity and not to instrumental causes. This circumstance also argues strongly against the suspicion that the apparent structure in the peaks arises from some influence of the atmospheric water bands in this region on the performance of the double-beam instrument.

The resolving power available in the region of the $(\nu_3 + \nu_1)$ combination band in liquid CS_2 did not permit resolution of detailed structure, but rough values of components could be estimated from the inflections in the band envelope. The absence of interfering atmospheric bands in this spectral region further removes any suspicion that the band structures are spurious.

(b) Bandwidths

The strength of the peak absorptions in the sulfur dioxide spectra prevented measurement of the bandwidths in the pure liquid, but it is quite certain that the bands were much narrower in the 10% solution in chloroform than in the pure liquid. The spectra for ν_1 and ν_3 of SO_2 also appear to indicate a narrowing of the bands at lower temperatures. The more definite results obtained for ν_2 are plotted in Figure 9 which indicates a linear decrease of the bandwidth at half maximum intensity with decreasing temperature.

In contrast to this result, no significant narrowing was observed for the ν_3 band of CS_2 as the temperature was lowered from 25°C to -50°C, either for the pure liquid or for solutions of 20% or 2% CS_2 in chloroform.

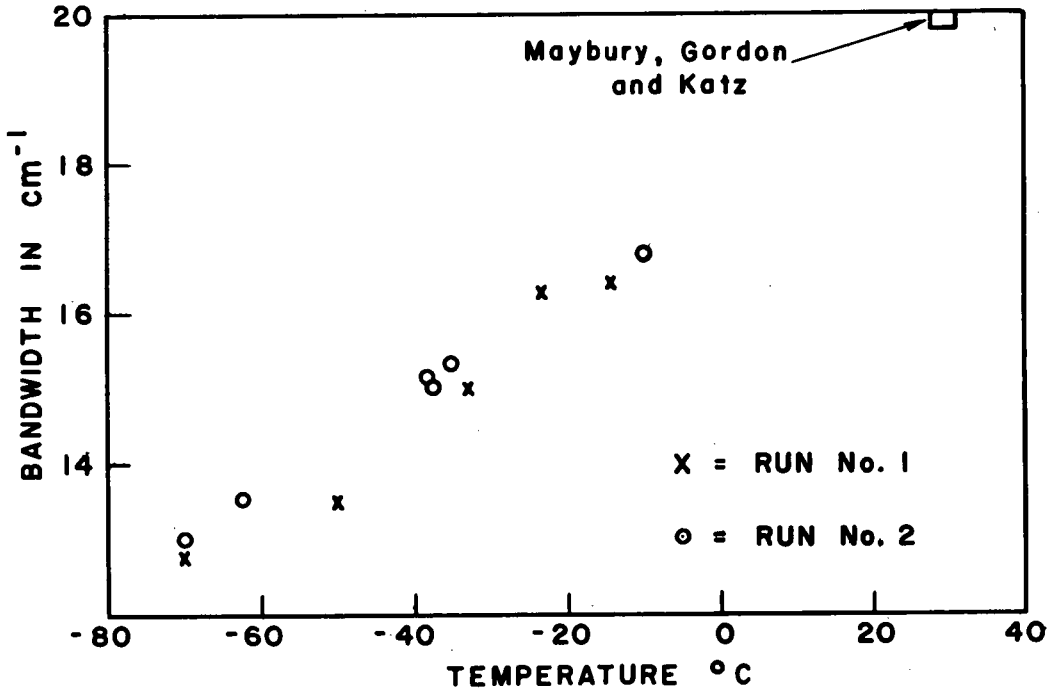

Figure 9. Temperature variation of the width at half maximum intensity for ν_{λ_2} of sulfur dioxide.

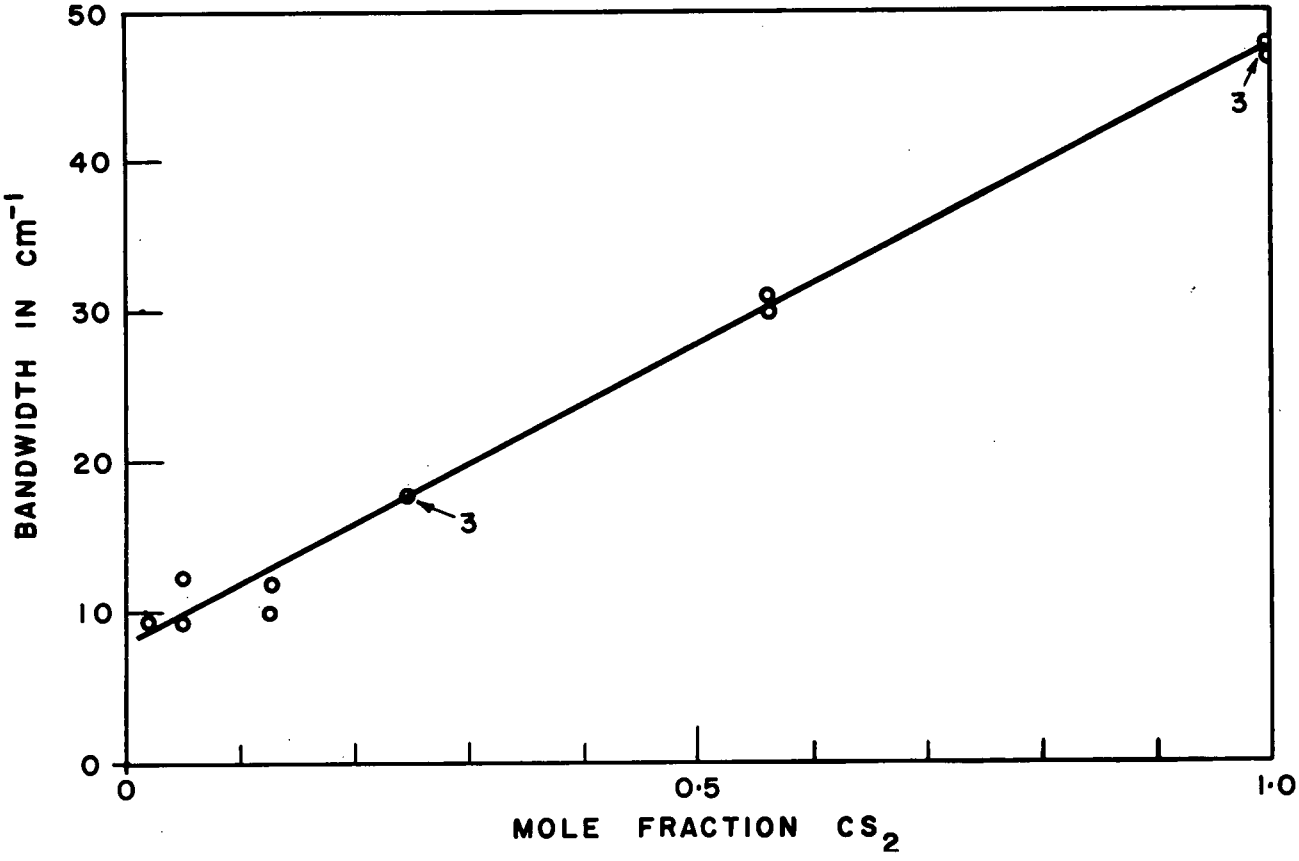

Figure 10. Variation with concentration of the width at half maximum intensity for ν_3 of carbon disulfide in solution in chloroform.

Dilution of CS_2 with $CHCl_3$ produced changes in the bandwidth of the absorptions in both the ν_3 and the ($\nu_3 + \nu_1$) regions. Results for ν_3, corrected for the effects of finite slit width, are presented in Figure 10. The bandwidth of ν_3 at half maximum intensity is seen to vary in a closely linear fashion with the mole fraction of CS_2 over a range from 47 cm^{-1} in the pure liquid to less than 10 cm^{-1} in dilute solution. A few observations on solutions of CS_2 in CCl_4 gave bandwidths indistinguishable from those in $CHCl_3$ solutions of the same mole fraction. The variation in bandwidth was less marked for ($\nu_3 + \nu_1$), which ranged from 29 cm^{-1} in the pure liquid to 20 cm^{-1} in a 20% solution.

(c) Intensities

It was not possible to measure the true integrated absorption coefficients for ν_3 and ν_1 of pure liquid sulfur dioxide. In the spectra obtained, the percent transmission at both peaks was still zero when a neutral density filter of wire mesh (optical density 0.68) was placed in the reference beam. This observation made possible a measure of a lower limit for the integrated absorption coefficient for ν_1, since the peak optical density must have been greater than 2.5. The result obtained was 2.9×10^3 $\ell.$ $mole^{-1}$ cm^{-2}, so that the intensity of ν_1 in the liquid was not less than 1.34 times the gas phase intensity in corresponding units. The formulas based on the Lorentz-Onsager treatment of dielectric polarization, which have been advanced by Chako (15) and Polo and Wilson (44), predict a value of 1.26 for this ratio. A similar calculation for ν_3 gave the lower limit in the liquid phase as roughly 1/2 the gas phase value, but the true intensity was probably much greater than this.

The intensity of ν_1 of SO_2 in a 10% solution in chloroform was determined to lie between 3.9×10^3 and 6.9×10^3 $\ell.$ mole^{-1} cm^{-2}, the uncertainty arising from the contribution of the neighboring chloroform band to the absorption in the region of ν_1. This places the ratio A_ℓ/A_g for the solution between the limits 1.5 and 2.7, as compared with 1.28 predicted on the basis of the Polo and Wilson formula.

Serious doubt attaches to the measurements made on ν_2 of SO_2 in view of the discovery that the cell was far from uniform in thickness. However, the internal consistency of the results as evidenced by the approximate agreement of the liquid and vapor phase intensities justifies their presentation. Figures 9 and 11 respectively present the variation of the apparent bandwidth and the apparent integrated absorption coefficient with temperature. Since the same absorption cell showed no significant temperature coefficient when filled with CS_2, it seems that the only possible source of this large temperature variation other than a real effect would be the presence in each trial of a vapor bubble in the cell which contracted on cooling. The effective cell thickness, evaluated using bands of known intensity, was 1.30 microns. When this value was applied to the band area at 25°C obtained by extrapolation, the integrated absorption coefficient obtained was roughly 3.5×10^3 $\ell.$ mole^{-1} cm^{-2}, which is about 1.4 times the gas phase intensity of ν_2, a figure very similar to that found for ν_1. This ratio would rise to 4.2 near the freezing point if the observed temperature coefficient was real.

The intensities of the three fundamentals of SO_2 all decreased dramatically when the liquid froze. The intensity changes were quantitatively reversed on melting. The behavior of ν_3 appeared to differ from

that of ν_2 in that very extensive wings of somewhat irregular contour developed on both sides of the central absorption. It is not certain whether such wings developed on ν_1, but from the symmetry of the wings on ν_3 it seems likely that they did not. The first explanation which suggests itself is scattering by the polycrystalline film, but the absence of any significant increase in scattering at frequencies far from the band centres suggests that these wings are properly considered as regions of absorption. On this assumption, the integrated absorption coefficient was evaluated over a frequency region from 1520 to 920 cm^{-1} which includes both ν_3 and ν_1, the value obtained being 6.35×10^3 $\ell.$ $mole^{-1}$ cm^{-2}. A separate integration for ν_1 on the further assumption that the wing absorption was due entirely to ν_3 gave 3.9×10^2 $\ell.$ $mole^{-1}$ cm^{-2}, in which case ν_3 would be 5.96×10^3 $\ell.$ $mole^{-1}$ cm^{-2} by difference. The ratios of the solid to the gas phase intensities on this basis are then 0.18 for ν_1 and 0.34 for ν_3. This ratio for the total absorption by ν_3 and ν_1 is 0.32.

The intensity decrease on freezing for the bending vibration, ν_2, was found to be 44%. Acceptance of the measured integrated absorption coefficient as correct at 4.9×10^3 $\ell.$ $mole^{-1}$ cm^{-2} for ν_2 of frozen SO_2 would give the intensity of this vibration in the solid as 3.2 times the gas phase value.

The measured intensities for ν_3 of CS_2 in the liquid phase present another anomalous situation. The integrated absorption coefficients for ν_3 in pure liquid CS_2 and in solution in $CHCl_3$ or CCl_4 are plotted in Figure 12 as a function of the mole fraction of CS_2. Corrections for the effect of finite slit width have been applied by the methods

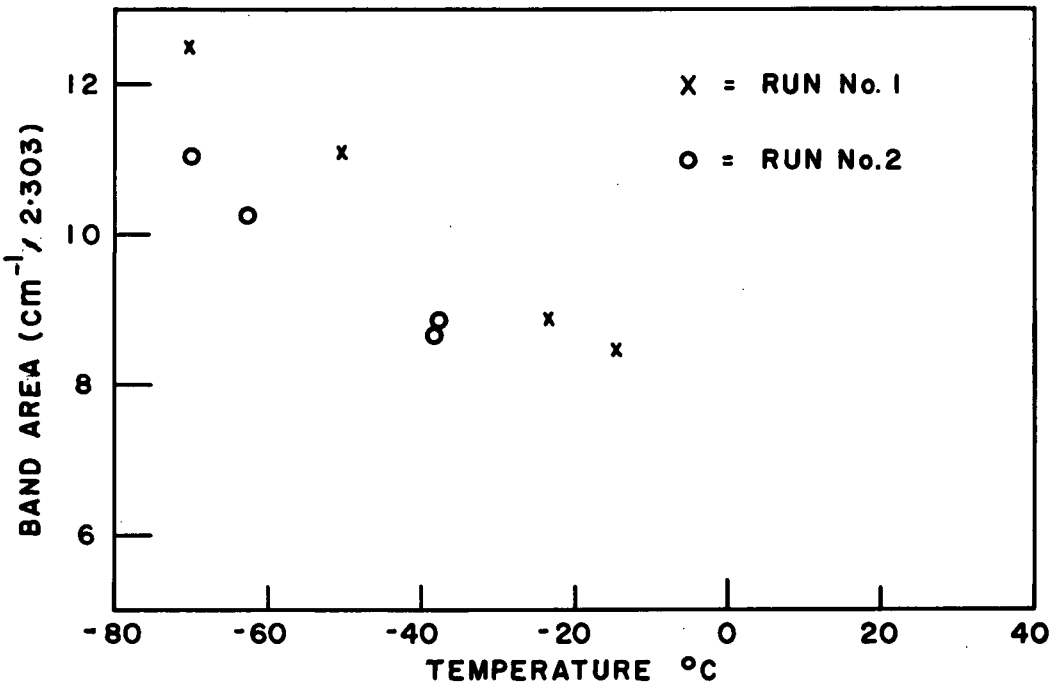

Figure 11. Temperature variation of the apparent integrated absorption coefficient for ν_2 of sulfur dioxide.

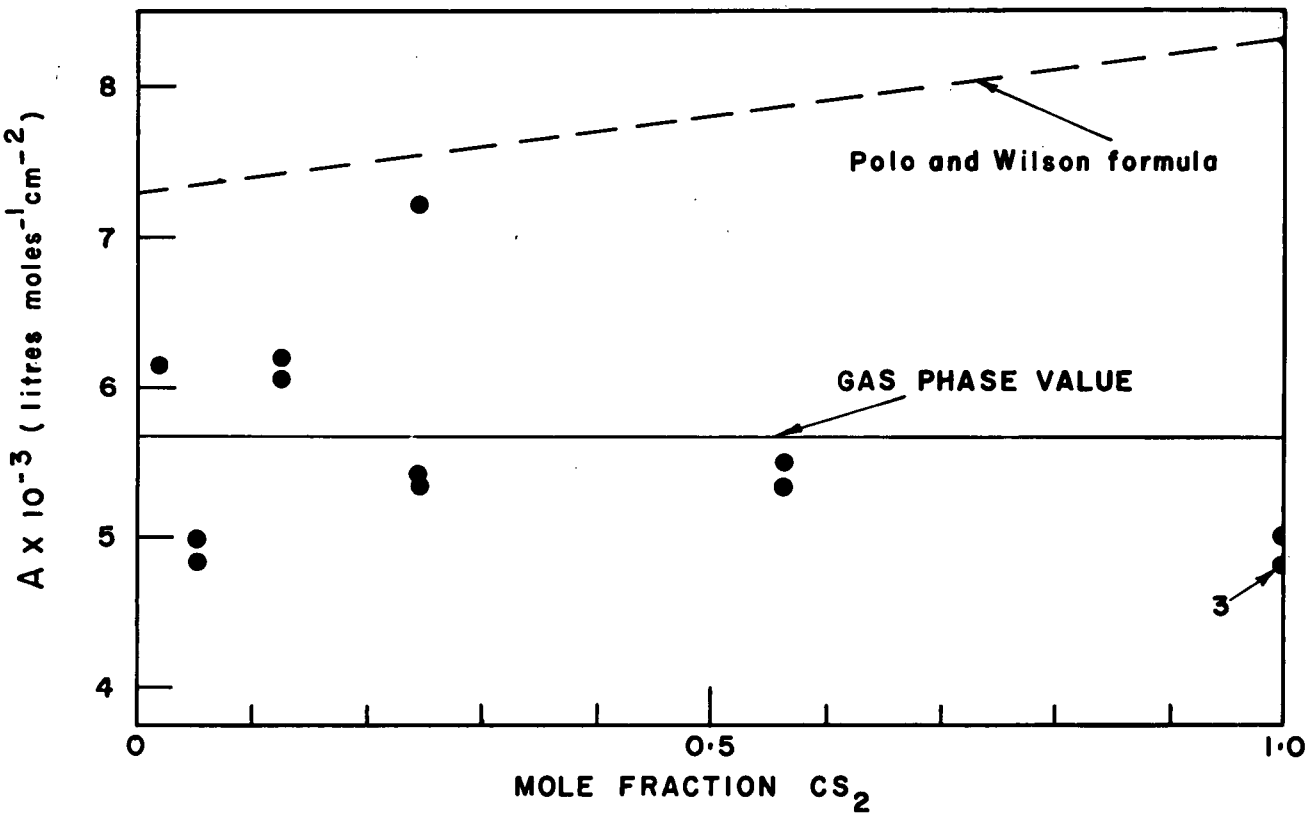

Figure 12. Variation with concentration of the true integrated absorption coefficient for ν_3 of carbon disulfide in solution in chloroform.

of Ramsay (47), ignoring the departures from Lorentz shape on the ground that they are of second-order importance.

No really significant variation of intensity with concentration can be inferred from Figure 12, though such variation might have been expected on the basis of the shape changes described above. The scatter is much greater than would be anticipated from the estimated errors in cell thickness, concentration, and area measurement, but is within the limits usually reported for this type of measurement. The gas phase intensity reported by Robinson (49) and by McKean, Callomon, and Thompson (36) is indicated by a horizontal line in Figure 12, while the intensity variation predicted on the theories of Chako (15) and Polo and Wilson (44) is indicated by the upper sloped line. The measured values fall well below the predicted ones, and seem to fall below the gas phase value, at least in the pure liquid.

Only a few measurements were made for other bands of CS_2. The gas phase intensity for $(\nu_3 + \nu_1)$ was obtained at four values of the partial pressure between 1.27 mm and 127 mm, and the B values were found to be constant within 10% over this range, indicating effectively zero slope for the B extrapolation. Thus A_g was found to be $(1.01 \pm .05) \times 10^3$ ℓ. mole^{-1} cm^{-2}. For pure liquid CS_2, A_ℓ was found to be 1.38×10^3 ℓ. mole^{-1} cm^{-2}. The ratio of these values, 1.37, agrees within the 10% uncertainty in this ratio with the figure 1.47 predicted from the Polo and Wilson formula.

CHAPTER V

DISCUSSION

1 The Absolute Intensities of the Sulfur Dioxide Fundamentals in the Vapor Phase

It will be noted that the intensities of the fundamentals of sulfur dioxide measured in this work differ from those reported by Eggers, Hisatsune, and Van Alten (19), being greater by 40, 45, and 60% for ν_1, ν_2, and ν_3 respectively. This disagreement has been discussed with Professor Eggers. The determination of band areas in the present work involved no replotting of data, and was less affected by instrument noise, so that the factor of personal judgment referred to in their paper was minimized here. The greater broadening pressures used in their work gave a truly linear variation of band area with partial pressure in the range of partial pressures used. Although the present work was conducted at much lower broadening pressures, the longer cell length permitted the use of much lower partial pressures so that adequate broadening was in fact achieved. Evidence obtained here (Table III) and elsewhere (14, 63) indicates that any inadequacy in the broadening should yield low values for the intensities, whereas our results are higher than those obtained by Eggers' group. The effects of incomplete mixing and adsorption were eliminated in both studies.

Thus a decision between the two sets of intensities rests upon the accuracy of the determination of the concentration of sulfur dioxide

in the absorption cell. In their work, refrigerant grade SO_2 was drawn directly from the can into the cell, and the mass spectrometric analysis was calibrated in terms of samples similarly prepared. Their analysis was thus a reliable test of adsorption loss, but was not necessarily an absolute measure of the SO_2 concentration. The non-condensable gas found in our cylinder of reagent grade SO_2 suggests a possible source of error in their analysis of nitrogen-SO_2 mixtures. Our purification procedure, quantitative recovery of the complete sample, and gravimetric determination of quantity should provide the more accurate determination of the SO_2 concentration, a conclusion to which Professor Eggers has subscribed. A further point in favor of the present results is that the curves of Figures 3, 4, and 5 all pass through the origin, whereas the ν_2 values reported by Eggers et. al. fail to conform to this essential requirement.

2 Bond Moments in Sulfur Dioxide

It was pointed out in Chapter II that the interpretation of infrared intensities in terms of bond moments involves a considerable number of assumptions, not all of which are above suspicion. It must, therefore, be borne in mind that the $\partial\vec{\mu}/\partial Q_k$ of Table IV are conditioned by the assumption that higher multipole moments and anharmonicity in the potential function are unimportant. In turn, the $\partial\mu/\partial S_i$ of Table V are conditioned by the selected form of the potential function and the empirical accuracy of the force constants, bond angle, and interatomic distance. The discussion which follows assumes that the $\partial\mu/\partial S_i$ are free of bias from these sources, and that only the later assumptions concerning bond moment additivity are under test.

It is seen in Table V that the dipole moment to be associated with the S - O bond in SO_2 on the basis of the measured intensity of ν_1 and ν_2 is $\mp$ 2.98 Debye if the signs of $\partial\mu/\partial Q_1$ and $\partial\mu/\partial Q_2$ are the same, or $\pm$ 3.12 Debye if they are different. The corresponding values for the total dipole moment of SO_2 are then $\mp$ 3.00 and $\pm$ 3.14 Debye respectively. If the assumptions behind these calculations are correct at least in the present case, one of these alternatives should agree with the total moment of 1.59 Debye obtained from the pure rotational spectrum (16) and from dielectric constant measurements (73).

The value of depends almost entirely on the intensity of ν_2 alone. The ν_2 data shows the greatest scatter of the three bands measured; the standard deviation about the least squares line is 4.5%. Thus a fair estimate of the standard error in determining μ from these data is $\pm$ 2.3%. It is therefore quite definite that the "dipole moment" calculated from the infrared intensities on the assumptions of the fixed-charge model is not the same quantity as the "static molecular dipole moment" measured by the other methods referred to above.

The failure of the fixed-charge model is further emphasized by a comparison of its other predictions with the results of Table V. A molecular orbital treatment of SO_2 by Moffitt (39) assigns formal charges of + 0.48 electrons to the sulfur atom and - 0.24 electrons to each oxygen. This charge distribution is consistent with the observed static dipole moment. Thus on the assumptions of the fixed-charge model we should find not only agreement of the μ values, but we should find $\partial\mu_{SO}/\partial r$ to be 0.24 electrons or about 1.0×10^{-10} esu independent of the symmetry class of the normal vibration. None of the alternatives of

Table V are in good agreement with this prediction. The signs of the derivatives may also be considered. Moffitt's formal charges give the positive sign for μ in the coordinate systems used here, and predict the positive sign for $\partial\mu/\partial S_1$ and the negative sign for $\partial\mu/\partial S_2$, so that the signs of $\partial\mu/\partial Q_1$ and $\partial\mu/\partial Q_2$ should also be taken as being different. This choice, however, leads to large disagreement of the value of $\partial\mu_{SO}/\partial r$ from ν_1 and ν_2 with that from ν_3. In studies on other molecules conclusions as to signs and magnitudes of derivatives have occasionally been based on the consistency argument that the magnitudes calculated from vibrations of different symmetry ought to agree. The accumulated evidence presented by Hornig and McKean (26) calls this procedure into question; the present evidence demonstrates that the procedure is inconsistent with the hypothesis used in the calculations.

The overall conclusion from these findings is that the amount of charge redistributed in the molecular distortions of sulfur dioxide is much greater than the formal charges of the equilibrium distribution. This suggests that the concepts of rehybridization, orbital following, and the contributions of unshared electrons which Hornig and McKean have applied successfully in NH_3 and HCN are needed for a discussion of the SO_2 intensities.

It has been shown that unshared pairs can make large contributions to the static moments (of the order of 1 Debye unit), and that they are very easily polarized (56). The molecular orbital calculations of Moffitt for sulfur dioxide and related compounds show that the sulfur unshared electrons occupy orbitals which are directed approximately

tetrahedrally with respect to the S - O bonds, and are pulled towards the oxygen atoms. Thus the unshared pair moment in the equilibrium configuration opposes the S - O bond moment. It is found that the configurations of the sulfones, R_2SO_2, are nearly tetrahedral while the S - O bond order is almost unaltered from its value in SO_2, and the dipole moment increases from 1.59 Debyes in SO_2 to more than 4 Debyes for dialkyl sulfones.

If we assume that the lone pair orbitals follow the motions of the oxygen atoms but otherwise retain the concepts of the fixed-charge model, qualitative consistency can be given to the signs and relative magnitudes of the moment derivatives in sulfur dioxide. Thus the lone pair moment, ordinarily in opposition to the bond moment but reduced in its effect by displacement of the lone pair orbitals towards the oxygens, would further decrease as the S - O bonds stretched slightly leading to an augmented positive change in μ for distortions of type S_1. Similarly, the opposition of the lone pair moment to the bond moment would increase for increases in the bond angle leading to an augmented negative value of $\partial\mu/\partial S_2$. Distortions according to S_3 would cause both bond and lone pair moment changes in the same direction leading to large positive values of $\partial\mu/\partial S_3$.

These suggestions should not be taken too seriously since they represent a gross oversimplification of the effects of molecular distortion. The consistency which they appear to give to the infrared data, and the success of similar arguments for NH_3 and HCN, call attention to the importance of unshared pairs in problems of molecular structure and to

the need for further investigation on both the empirical and theoretical behavior of these electrons. The pronounced sensitivity of infrared intensities to the details of the molecular charge distribution emphasizes their application as a tool in the study of molecular structure.

3 Frequencies, Bandwidths, and Intensities in the Liquid and Solid Phases

The results obtained on spectra in the liquid and solid phases present many interesting features. Unfortunately the scope of the experimental work is too limited to provide a solid basis for the interpretation of these features. The rather speculative discussion of these results which follows is intended primarily to suggest some directions which might be taken in future work.

The liquid-phase band contours found for the fundamentals of SO_2 were closely Lorentzian for the symmetric vibrations ν_1 and ν_2 in agreement with well-recognized concepts of the collision broadening of the vibrational levels, the rotational structure being suppressed by collision frequencies in excess of the rotation frequencies (47). In contrast, the asymmetric vibration, ν_3, showed a triplet structure which corresponded, not to the perpendicular band structure of the gas phase, but to the triplet structure observed in the solid at temperatures near the melting point. There was no obvious temperature coefficient found for the relative intensities in this structure. The similar, though more complex, structure found in the analogous vibration (ν_3) of CS_2 also showed no temperature coefficient beyond that expected from thermal contraction of the liquid over a 75°C range. At least some of the components of the latter peak appear to correspond to frequencies observed in the Raman

spectrum of frozen CS_2. Both triplet structures referred to disappeared or were modified in chloroform solutions.

None of the three SO_2 vibrations showed a significant frequency shift on freezing, though the previously reported shifts (downward for ν_1 and ν_3, upward for ν_2) from the gas frequencies were confirmed in the liquid. However, large decreases in intensity of all three bands occurred on freezing, and several weak sidebands appeared.

The first idea suggested by these observations is that the triplet structure in ν_3 of SO_2 found in both the solid and liquid states, but disappearing in solution, represents the resonance splitting of oscillators coupled by the crystalline field of the solid, as discussed by many authors including Hornig (25) and Wiener and Nixon (69). The work of these authors indicates that only ν_3 should show such splitting, which is what is observed if the other weak sidebands in the regions of ν_2 and ν_1 are assumed to arise from second order or spurious causes. This hypothesis accounts for two components of the ν_3 structure, though it is not certain which two. If the third component is assumed to arise from "free" molecules, then it is presumably the central component at about 1336 cm^{-1}, since it is this frequency which remains in the solution. Whatever the proper identity of these components, their assignment as characteristic of the solid lattice seems unavoidable. The overall weakness of the bands in the solid state, together with the observed persistence of the triplet structure at temperatures 30 degrees or more above the melting point suggest that a marked degree of essentially crystalline structure exists in the liquid at these temperatures. If by analogy it is assumed that the multicomponent structure of ν_3 of CS_2 is

characteristic of the solid lattice (there is some slight support for this from Raman studies (30, 34, 54)), then the persistence of crystalline structure is truly remarkable in liquid CS_2, since no temperature change greater than 10% was observed between -50°C and 25°C.

The idea that liquids possess regions of local order comparable to that of the solid lattice is supported by evidence from X-ray diffraction (57) and light scattering (23). If it is assumed that the lattice stabilization energy is large with respect to kT, only a very small proportion of collisions will occur at energies sufficient to remove a molecule from, or to split, a "crystallite". For equilibrium to hold it is necessary that an equally small proportion of collisions should lead to growth of crystallites, and since the fraction of collisions energetically favorable to crystallization is large by the assumption already made, the "accommodation coefficient" must be much less than unity. This condition would be satisfied if a narrowly defined orientation were required for a molecule approaching a crystallite in order that the lattice stabilization energy be realized. While such concepts are a familiar part of discussions of crystallization phenomena (75) the majority of calculations on intermolecular forces treat the intermolecular potential function as spherically symmetric or ellipsoidal. The general inadequacy of such calculations in accounting for the properties of matter (77) indicates the need for more refined information on intermolecular forces. The argument advanced above suggests that infrared studies of temperature changes and phase transitions may be valuable avenues of approach to such information.

The results of the present work on frequencies and intensities

in the liquid phase are not well accounted for by the essentially macroscopic approach of theories of dielectric polarization. These theories, which were discussed briefly in Chapter II, predict that all frequencies of a molecule should decrease and all band intensities should increase when the phase change from gas to liquid occurs. The fact that the frequency of ν_2 of SO_2 increases is in itself sufficient to indicate that the macroscopic approach is unlikely to lead to an adequate understanding of molecular interactions. Upward shifts in frequency have been reported by other workers (9, 76). The measured liquid intensities for ν_3 of CS_2 appear to be significantly below the predictions of the dielectric polarization theories, while the intensities of ν_1 and ν_3 of SO_2 in chloroform solution and ν_1 in the pure liquid appear to be significantly greater than predicted. The data of Whiffen (68) on the intensity of the C - Cl stretching vibration of chloroform in various solvents did not correlate well with the Chako formula. While these few results by no means serve to define the limits of application of the approach through the theory of dielectric polarization, it does not seem likely that this approach will be any more adequate for the problem of intensities than it is for frequencies (22, 51).

Finally, the measured bandwidths in this work indicate a potentially valuable field of study. The more than four-fold reduction in the bandwidth of ν_3 of CS_2 on going from the pure liquid to dilute solutions show that this particular vibration is more strongly influenced by collisions between like molecules than between unlike molecules. This is supported by a kinetic theory estimate of the collision frequency which is higher by about 50% for a CS_2 molecule in essentially pure

chloroform than in pure CS_2. Moreover, if collision frequency were the principal determinant of bandwidth, the width should vary as the square root of the absolute temperature; our data for pure CS_2 and 2% solution in $CHCl_3$, though of marginal accuracy, do not support so large a temperature coefficient.

It should be noted that Brown (12) has extrapolated this kinetic theory approach to bandwidth to predict that the integrated absorption coefficient should vary with temperature for a Lorentz band. The argument on which he bases this conclusion appears to be in error. Starting from the Lorentz-type equation given by Ramsay (47),

$$\ln \frac{I_o}{I} = \frac{a}{(\nu - \nu_o)^2 + b^2}$$

Brown assumes that "a" is a constant, independent of temperature, while "b", defined by the relation

$$2b = \Delta\nu_{1/2}$$

is taken on kinetic theory grounds (see p. 15) to vary as $T^{1/2}$. He then performs the integration

$$\int_{-\infty}^{\infty} \ln \frac{I_o}{I}\, d\nu = \int_{-\infty}^{\infty} \frac{a}{(- \ _o)^2 + b^2}\, d\nu = \frac{\pi a}{b} = \frac{2\pi a}{\Delta\nu_{1/2}}$$

from which he concludes that the integrated area must vary as $T^{-1/2}$. The point of fallacy here is that the quantity "a" is defined by this integration, and in the theory of collision broadening (78, 18, 40) is shown to consist of the integrated area times b/π. Thus the assumption that "a" is temperature invariant is completely unwarranted. The only defensible a priori assumption is that the transition probability (and

thus the integrated absorption coefficient) is not temperature dependent, and to regard departures from this behavior as evidence for the temperature dependence of the intermolecular forces.

The linear form observed for the dependence of bandwidth on mole fraction requires comment. If the band contour observed in a solution were the sum of contributions from molecules subject to perturbation by a single nearest neighbor of like species and from molecules similarly perturbed by a neighbor of unlike species, it is easily shown that the dependence of bandwidth on mole fraction would not be linear in form. An alternative hypothesis leading to a linear form is that the bandwidth is determined by some intensive property of the solution, for which refractive index might be suggested in a macroscopic view, or the average electric field at the absorbing molecule due to all the other molecules in a microscopic view. The latter concept is akin to the London dispersion-force model (77). It is not impossible to account for the linear form of the bandwidth-concentration curve in terms of the "crystallite" model discussed in connection with the frequencies, but several assumptions are required concerning which no evidence is available. Thus the only proper conclusions from the measurements on CS_2 solutions, and the corroborative observations on SO_2 solutions, are that they are consistent with the usual chemical rule-of-thumb (52) that interactions are stronger between like than between unlike molecules, and that bandwidth variations with concentration and temperature merit more detailed investigation.

SUMMARY

Measurements have been made of the absolute intensities of the three fundamental vibration-rotation bands of sulfur dioxide vapor. The measurements are different from previously published values and are shown to be preferable to them. The measured intensities thus provide the best standard yet available against which to test theories of infrared intensities and molecular charge distribution. The molecular model employed almost exclusively up to the present time has been shown to be inadequate for the interpretation of the sulfur dioxide intensities, the effective oscillating charges being considerably larger than the formal charges of the equilibrium configuration. The involvement of unshared electrons in both the equilibrium and distorted charge distributions is strongly suggested by the results obtained.

Observations of limited scope on the shapes, frequencies, widths, and intensities of absorption bands in the solid and liquid states at various temperatures have shown that the predictions of the theory of dielectric polarization do not appear to provide an adequate description of the spectral changes accompanying a change of phase. Variation of bandwidth with concentration was demonstrated for solutions of CS_2 and SO_2 in organic solvents, and variations of bandwidth and intensity with temperature was observed in some cases but not in others. Both the latter findings are opposed to the hypothesis that collision frequency is the major determinant of bandwidth in the liquid state. Frequency structures

observed in the liquid state appeared to correspond to those observed in the solid state, suggesting that further studies might yield information on the degree of order present in liquids.

Note Added in Proof

It has been brought to my attention that results confirming the findings of this thesis for the sulfur dioxide vapor intensities have been obtained independently by J. Morcillo and J. Herranz (An. Real. Soc. Esp. Fis. Quim. 52A, 207, 217 (1956)). This journal is not yet available to us, but their results have been given in "Spectroscopia Molecular" Vol. 6, p. 9, February 1957. They are, in the same units as those of Table IV, p. 37:

$$A_1 = 350 \pm 20$$

$$A_2 = 360 \pm 30$$

$$A_3 = 2640 \pm 80.$$

The values for A_2 and A_3 agree within the limits of the errors in either investigation, while the A_1 values differ by the sum of the errors quoted. In view of the order of accuracy obtained in most studies of this kind, the agreement must be regarded as very satisfactory.

BIBLIOGRAPHY

1. Adams, R.M., and Katz, J.J. J. Opt. Soc. Am. 46, 895 (1956).

2. Anderson, P.A. Phys. Rev. 76, 647 (1949).
   Phys. Rev. 80, 511 (1950).

3. Aroeste, H. J. Chem. Phys. 22, 1273 (1954).

4. Barrow, G.M. J. Phys. Chem. 59, 1129 (1955).

5. Bauer and Magat. J. Phys. et le Radium 9, 319 (1938).

6. Benedict, W.S., Herman, R., Moore, G.E., and Silverman, S. Canad. J. Phys. 34, 830, 850 (1956).

7. Benesch, W., and Elder, T. Phys. Rev. 91, 308 (1953).

8. Bernstein, H.J. J. Chem. Phys. 8, 410 (1940).

9. Bernstein, R.B., and Tamres, M. J. Chem. Phys. 23, 2201 (1955).

10. Bourgin, D.G. Phys. Rev. 29, 794 (1927).

11. Brandt, W. J. Chem. Phys. 24, 501 (1956).

12. Brown T.L. J. Chem. Phys. 24, 1281 (1956).

13. Buckingham, A.D. J. Chem Phys. 23, 2370 (1955).

14. Callomon, H.J., McKean, D.C., and Thompson, H.W. Proc. Roy. Soc. (London). A 208, 332, 341 (1951).

15. Chako, N.Q. J. Chem Phys. 2, 644 (1934).

16. Crable, G.F., and Smith, W.V. J. Chem. Phys. 19, 502 (1951).

17. Crawford, B.L., and Dinsmore, H.L. J. Chem. Phys. 18, 983, (1950).
    J. Chem. Phys. 18, 1682, (1950).

18. Dennison, D.M. Phys. Rev. 31, 503 (1928).

19. Eggers, D.F. Jr., Hisatsune, I.C., and Van Alten, L. J. Phys. Chem. 59, 1124 (1955).

20. Fahrenfort, J., and Ketelaar, J.A.A. J. Chem. Phys. 22, 1631 (1954).

21. Fahrenfort, J. Thesis. University of Amsterdam, 1955.

22. Greinacher, E., Luttke, W., and Mecke, R. Z. fur Electrochemie. 59, 23 (1955).

23. Gross, E., and Vuks, M. J. de Phys. et le radium. 6, 467 (1935). 7, 113 (1936).

24. Hooge, F.N. Thesis. University of Amsterdam, 1956.

25. Hornig, D.F. Discussions of the Faraday Soc. 9, 115 (1950).

26. Hornig, D.F., and McKean, D.C. J. Phys. Chem. 59, 1133 (1955).

27. Howard, J.N., Burch, D.E., and Williams, D. J. Opt. Soc. Am. 46, 186 (1956).

28. Hughes, R..H., Martin, R.J., and Coggeshall, N.D. J. Chem. Phys. 24, 489 (1956).

29. Josien, M.-L., and Fuson, N. J. Chem. Phys. 22, 1169 (1954).

30. Kastha, G.S. Indian J. Phys. 29, 474 (1955).

31. Ketelaar, J.A.A., and Hooge, F.N. J. Chem. Phys. 23, 749, 1549 (1955).

32. Kivelson, D. J. Chem. Phys. 22, 904 (1954).

33. Lord, R.C., Nolin, B., and Stridham, H.D. J. Am. Chem. Soc. 77, 1365 (1955).

34. Majundar, . Indian J. Phys. 23, 2439 (1955).

35. Maybury, R.H., Gordon, S., and Katz, J.J. J. Chem. Phys. 23, 1277 (1955).

36. McKean, D..C., Callomon, H.J., and Thompson, H.W. J. Chem. Phys. 20, 520 (1952).

37. McKean, D.C., and Schatz, P.N. J. Chem. Phys. 24, 316 (1956).

38. Mecke, R. J. Chem. Phys. 20, 1935.(1952).

39. Moffitt, W. Proc. Roy. Soc. (London). A 200, 409 (1950).

40. Nielsen, J.R., Thornton, V., and Dale, E.B. Rev. Mod. Phys. 16, 307 (1944).

41. Onsager, L. J. Amer. Chem. Soc. 58, 1486 (1936).

42. Penner, S.S., and Weber, D. J. Chem. Phys. 19, 807 (1951).
19, 817 (1951).
19, 974 (1951).
21, 649 (1953).

43. Polo, S.R., and Wilson, M.K., J. Chem. Phys. 22, 900 (1954).

44. Polo, S.R., and Wilson, M.K. J. Chem. Phys. 23, 2376 (1955).

45. Polo, S.R. J. Chem. Phys. 24, 1133 (1956).

46. de Prima, C.R., and Penner, S.S. J. Chem. Phys. 23, 757 (1955).

47. Ramsay, D.A. J. Am. Chem. Soc. 74, 72 (1952).

48. Richards, and Burton. Trans. Faraday Soc. 45, 874 (1949).

49. Robinson, D.Z. J. Chem. Phys. 19, 881 (1951).

50. Rollefson, R., and Havens, R. Phys. Rev. 57, 710 (1940).

51. Ross, W.L. Thesis. University of British Columbia (1954).

52. Rowlinson, T.G. Quart. Rev. of Chem. Soc. (London). 8, 168 (1954).

53. Shelton, R.D., Nielsen, A.H., and Fletcher, W.H. J. Chem. Phys. 21, 2178 (1953).

54. Sirkar, S.C., and Kastha, G.S. J. Chem. Phys. 23, 2439 (1955).

55. Slowinski, E.J., and Claver, G.C. J. Opt. Soc. Am. 45, 396 (1955).

56. Smyth, C.P. J. Phys. Chem. 59, 1121 (1955).

57. Stewart, G.W. Phys. Rev. 30, 232 (1927).
31, 174 (1928).
35, 726 (1930).
37, 9 (1931).

58. Stuart, A.V. J. Chem. Phys. 21, 1115 (1953).

59. Thorndike, A.M., Wells, A.J., and Wilson, E.B. Jr. J. Chem. Phys. 15, 157 (1947).

60. Thorndike, A.M. J. Chem. Phys. 15, 868 (1947).

61. Vincent, J. J. de Phys. et le Radium. 11, 1 (1950).

62. Vincent-Geisse, J. J. de Phys. et le Radium. 17, 63 (1956).

63. Welsh, H.L., Pashler, P.E., and Dunn, A.F. J. Chem. Phys. 19, 340 (1951).

64. Welsh, H.L., and Sandiford, P.J. J. Chem. Phys. 20, 1646 (1952).

65. Welsh, H.L., Pashler, P.E., and Stoicheff, B.P. Canad. J. Phys. 30, 99 (1952).

66. West, W. J. Chem. Phys. 7, 795 (1939).

67. West, W., and Edwards. J. Chem. Phys. 5, 14 (1937).

68. Whiffen, D.H. Trans. Faraday Soc. 49, 878 (1953).

69. Wiener, R.N., and Nixon, E.R. J. Chem. Phys. 25, 175 (1956).

70. Wilson, E.B. Jr. J. Chem. Phys. 7, 1047 (1939).
9, 76 (1941).

71. Wilson, E.B. Jr., and Wells, A.J. J. Chem. Phys. 14, 578 (1946).

Books

72. Bellamy, L.J. Infrared Spectra of Complex Molecules. London, Methuen and Co. Ltd., 1954.

73. Brown, William Fuller Jr. Dielectrics. Vol. XVII of Encyclopedia of Physics. Berlin, Springer-Verlag, 1956.

74. Debye, P. Polar Molecules. New York, Chemical Catalogue Co., Inc., 1929.

75. Frenkel, J. Kinetic Theory of Liquids. Oxford, Clarendon Press, 1946.

76. Herzberg, G. Molecular Spectra and Molecular Structure. Toronto, D. Van Nostrand Co. Inc., 1945, vol. II.

77. Hirschfelder, J.O., Curtiss, C.F., and Bird, R.B. Molecular Theory of Gases and Liquids. New York, John Wiley and Sons, Inc., 1954.

78. Lorentz, H.A. Theory of Electrons. Leipzig, Teubner, 1909.

79. Unsold. Physik der Sternatmosphären. Berlin, Julius Springer, 1938.

80. Vogel, A.I. Quantitative Inorganic Analysis. Toronto, Longmans-Green and Co., 1951, 2nd ed.

81. Wilson, E.B. Jr., Decius, J.C., and Cross, P.C. Molecular Vibrations. Toronto, McGraw Hill Book Co. Inc., 1955.

APPENDIX I

NORMAL COORDINATE TREATMENT FOR SULFUR DIOXIDE

The principles and methods involved in relating the vibrational motions of a molecule to any desired set of internal coordinates have been summarized by Wilson, Decius, and Cross (81). Their notation has been used in what follows. The application of these methods to the sulfur dioxide molecule has been carried out by Eggers, Hisatsune, and Van Alten (19). The treatment below includes some details omitted from these publications and points out some problems which arise in the solution.

1 General Relations

We proceed on the basis that all equations contained in Molecular Vibrations by Wilson, Decius, and Cross are available. It is there shown (Appendix VIII) that if $\underline{L}$ is the matrix of coefficients which transform any set of internal coordinates represented by the column matrix $\underline{S}$ into the column matrix of the normal coordinates, $\underline{Q}$, according to

$$\underline{S} = \underline{L}\underline{Q} \tag{1}$$

then the matrix $\underline{L}^{-1}$ of coefficients for the inverse transformation

$$\underline{Q} = \underline{L}^{-1}\underline{S} \tag{2}$$

may be obtained as follows.

The normal coordinates are defined to be such that the kinetic energy T and the potential energy V are given in diagonal form (no cross-products between coordinates),

$$2V = \underline{Q}^{\dagger} \underline{\Lambda} \underline{Q} \tag{3}$$

$$2T = \dot{\underline{Q}}^{\dagger} \underline{E} \dot{\underline{Q}} \tag{4}$$

where the dot refers to the time derivative, the dagger indicates the transpose conjugate, $\underline{E}$ is the unit matrix, and $\underline{\Lambda}$ is the diagonal matrix whose elements are $\lambda_k = 4\pi^2\nu_k^2$ where ν_k is the frequency of the normal vibration in which the distortion is specified by the normal coordinate Q_k. The Q's may thus be described as mass-weighted displacement coordinates.

It is also shown there that the potential and kinetic energies are related to the internal coordinates $\underline{S}$ by the relations

$$2V = \underline{S}^{\dagger} \underline{F} \underline{S} \tag{5}$$

$$2T = \dot{\underline{S}}^{\dagger} \underline{G}^{-1} \dot{\underline{S}} \tag{6}$$

In these expressions $\underline{F}$ is the matrix of the force constants, the construction of which is discussed below, and $\underline{G}^{-1}$ is the "inverse G matrix" for which Equation (6) is essentially the defining equation, and which is constructed from the atomic masses and geometry of the molecule.

Combining (1) with (5) and (6) we have

$$2V = \underline{Q}^{\dagger} \underline{L}^{\dagger} \underline{F} \underline{L} \underline{Q} \tag{7}$$

$$2T = \dot{\underline{Q}}^{\dagger} \underline{L}^{\dagger} \underline{G}^{-1} \underline{L} \dot{\underline{Q}} \tag{8}$$

Comparison with (3) and (4) gives

$$\underline{L}^{\dagger}\,\underline{F}\,\underline{L} = \underline{\Lambda} \tag{9}$$

$$\underline{L}^{\dagger}\,\underline{G}^{-1}\underline{L} = \underline{E} \tag{10}$$

Equation (10) may be solved to give $\underline{L} = G(L^{-1})^{\dagger}$ which may be substituted in Equation (9); multiplication by $(L^{-1})^{\dagger}$ then gives

$$\underline{F}\,\underline{G}\,(\underline{L}^{-1})^{\dagger} = (\underline{L}^{-1})^{\dagger}\underline{\Lambda} \tag{11}$$

As will be seen below, this equation may be used to obtain the ratios of the coefficients L^{-1}_{ki} which coefficients are just the quantities $\partial Q_k/\partial S_i$ required in Equation (7) of Chapter II. In order to fix the values of these coefficients a second condition is required. This may be obtained from either (9) or (10). Since the elements of the G matrix are more accurately known than those of the F matrix, the latter course has been preferred here. From (10) we obtain

$$\underline{L}^{-1}\underline{G}\,(\underline{L}^{-1})^{\dagger} = \underline{E} \tag{12}$$

There is moreover a condition of compatibility on the set of linear equations defined by Equation (11), which is that

$$|FG - E\Lambda| = 0 \tag{13}$$

This is one form of the secular equation of the molecule, from which the frequencies may be calculated if the F matrix is known. More usually the frequencies are measured and the force constants, which in general outnumber the frequencies, are adjusted to give agreement between the observed frequencies and those calculated from Equation (13).

2 Application to Sulfur Dioxide

The potential function for the sulfur dioxide molecule may be written in its most general quadratic form as

$$2V = f_r(\Delta r_1^2 + \Delta r_2^2) + f_\theta r^2 \Delta\theta^2 + 2f_{rr}\Delta r_1 \Delta r_2 + 2f_{r\theta} r(\Delta r_1 + \Delta r_2)\Delta\theta \qquad (14)$$

Here Δr_1 and Δr_2 are changes in the S - O bond length, r is the equilibrium bond length, and $\Delta\theta$ is the change in the O - S - O bond angle. If the symmetry coordinates of Equation (8), Chapter II are substituted into (5), comparison with (14) shows that the F matrix has the form

$$\underline{F} = \begin{bmatrix} f_r + f_{rr} & \sqrt{2}f_{r\theta} & 0 \\ \sqrt{2}f_{r\theta} & f_\theta & 0 \\ 0 & 0 & f_r - f_{rr} \end{bmatrix} \qquad (15)$$

The force constants have been evaluated by Polo and Wilson (43) and Kivelson (32) using combined infrared and microwave data. They are:

$$\begin{aligned} f_r &= 10.006 \text{ millidynes/angstrom} \\ f_{rr} &= 0.0236 \quad " \quad " \\ f_{r\theta} &= 0.189 \quad " \quad " \\ f_\theta &= 0.7933 \quad " \quad " \end{aligned} \qquad (16)$$

The G matrix has been given by Polo and Wilson (43). After adjusting for the choice of $S_2 = r\Delta\theta$ rather than $S_2 = \Delta\theta$ as in their work, the G matrix is

$$G = \begin{bmatrix} [\mu_o + (1 + \cos\theta)\mu_s] & -\sqrt{2}\sin\theta\,\mu_s & 0 \\ -\sqrt{2}\sin\theta\,\mu_s & 2[\mu_o + (1 - \cos\theta)\mu_s] & 0 \\ & & [\mu_o + (1 - \cos\theta)\mu_s] \end{bmatrix} \tag{17}$$

in which μ_o and μ_s are the reciprocal masses of the oxygen and sulfur atoms respectively. Using the molecular constants as given by Kivelson (32),

$$\mu_o = \frac{1}{16.00}\ \text{amu}^{-1} \quad \text{and} \quad \mu_s = \frac{1}{31.98}\ \text{amu}^{-1}$$

$$r = 1.4321\ \text{A} \quad \text{and} \quad \theta = 119.53^\circ$$

$$1\ \text{angstrom} = 10^{-8}\ \text{cm}$$

$$1\ \text{amu}^{-1} = 6.025 \times 10^{23}\ \text{gm}^{-1}$$

Substitution of these values gives the product matrix FG in the form

$$FG = \begin{bmatrix} 4.6728 & -1.9738 & 0 \\ -0.05778 & 0.98171 & 0 \\ 0 & 0 & 6.566 \end{bmatrix} \tag{18}$$

where the units of $(FG)_{tt'}$ are $10^{28}\ \text{sec}^{-2}$. From the observed frequencies with $\lambda_k = 4\pi^2 \nu_k^2$ we find

$$\underline{\Lambda} = \begin{bmatrix} 4.708 & 0 & 0 \\ 0 & 0.9572 & 0 \\ 0 & 0 & 6.581 \end{bmatrix} \tag{19}$$

where the units of λ_k are also $10^{28}\ \text{sec}^{-2}$. If we now apply the compatibility condition of Equation (13), we find that the determinant

$$|FG - E\Lambda| \neq 0$$

so that the force constants and frequencies used are not strictly compatible. However they are very nearly so, and the discrepancies have only a small effect on the L_{ki}^{-1} .

The ratios of the coefficients L_{ki}^{-1} may be obtained by expansion of Equation (11) to give the following relations

$$\frac{L_{11}^{-1}}{L_{12}^{-1}} = -\frac{(FG)_{12}}{FG_{11} - \lambda_1} = -\frac{(FG)_{22} - \lambda_1}{FG_{21}} = n_1 \qquad (20)$$

$$\frac{L_{21}^{-1}}{L_{22}^{-1}} = -\frac{(FG)_{12}}{FG_{11} - \lambda_2} = -\frac{(FG)_{22} - \lambda_2}{FG_{21}} = n_2 \qquad (21)$$

Expansion of Equation (12) then gives the relations

$$(L_{12}^{-1})^{-2} = n_1^2 G_{11} + 2n_1 G_{12} + G_{22} \qquad (22)$$

$$(L_{22}^{-1})^{-2} = n_2^2 G_{11} + 2n_2 G_{12} + G_{22} \qquad (23)$$

$$(L_{33}^{-1})^{-2} = G_{33} \qquad (24)$$

Alternative values of n_1 and n_2 are obtained from (20) and (21). These values would be identical if condition (13) were exactly satisfied. In fact the difference is of relatively small importance; moreover, error can be minimized by choosing the values of n which involve predominantly the best known terms of the F matrix, F_{11} and F_{22}. Applying this criterion we obtain from (20) to (24) inclusive,

$$L_{11}^{-1} = \pm\ 0.457 \times 10^{-11}\ gm^{1/2}$$

$$L_{12}^{-1} = \mp\ 0.00708 \times 10^{-11}\ gm^{1/2}$$

$$L_{21}^{-1} = \pm\ 0.153 \times 10^{-11}\ gm^{1/2} \qquad (25)$$

$$L_{22}^{-1} = \pm\ 0.288 \times 10^{-11}\ gm^{1/2}$$

$$L_{33}^{-1} = \pm\ 0.390 \times 10^{-11}\ gm^{1/2}$$

These values agree with those given by Eggers, Hisatsune and Van Alten (19). The ambiguities of sign are readily removed on physical grounds, since Q_1 must be predominantly S_1 and so forth, so that all the coefficients are positive except L_{12}^{-1}. The units ($gm^{1/2}$) of the coefficients are consistent with the requirements of Equation (2), since they convert the displacement coordinates S_i (units in cm) to the mass-weighted displacement coordinates Q_k (units in $gm^{1/2}cm$).

APPENDIX II

SPURIOUS MAXIMA IN COMPENSATED SPECTRA OF SOLUTIONS

It is general practice in double-beam infrared spectroscopy to remove solvent bands from the recorded spectrum of the solution by placing in the reference beam a thickness of pure solvent equivalent to that present in the sample beam. In the course of some studies on simultaneous vibrational transitions in liquid mixtures, it was noted that exact compensation was difficult to achieve since spurious maxima and minima appeared in the trace in the region of the compensated solvent bands. These "residual curves" occur because of small differences of the frequency, bandwidth, and intensity of an absorption band in the solution from their values in the pure solvent. Since a major object of the present work was to obtain information on just such effects as an indication of intermolecular forces, some attention was given to the problem of using these residual curves for this purpose. The final result was not promising, so that there is no point in reproducing here the many formulae which were derived and tested. A qualitative discussion of the approach made will suffice to outline the essential features of the problem.

The equation of the residual curve may be written down in terms of the equations of the absorption bands in the pure solvent and in the solution and the fact that the double-beam instrument records the ratio of the transmissions in the two beams. Many bands in the liquid phase have been found to be symmetrical and to conform to the Lorentz band

shape as modified by the effects of finite slit width (47) or to a Gaussian shape (48), over most of the central region of the band. If one or other of these forms is adopted, a definite form for a band can be written in terms of three parameters - the frequency, the halfwidth, and either the peak height or the integrated area of the band. The equation for the residual curve thus contains six parameters. For example, suppose the Lorentz formula is taken for the band shape

$$\ln \frac{I_o}{I} = \frac{a}{(\nu - \nu_o)^2 + b^2}$$

where ν_o is the central frequency, 2b is the bandwidth at half maximum intensity, and $a = b^2 \ln(I_o/I)_{\nu_o}$ is a measure of the band intensity. Then if in solution the frequency changes from ν_o to $(\nu_o + \gamma)$, the bandwidth changes from b to εb, and the intensity changes from a to αa, the equation of the residual curve becomes, putting $(\nu - \nu_o) = \delta$

$$\ln\left(\frac{T_S}{T_R}\right)_\delta = a\left\{\frac{(1-\alpha)\delta^2 - 2\gamma\delta + \gamma^2 + (\varepsilon^2 - \alpha)b^2}{[\delta^2 + b^2][(\delta - \gamma)^2 + \varepsilon^2 b^2]}\right\}$$

and the condition for a maximum or a minimum in the residual curve at a frequency δ_m is

$$\gamma^2\delta_m - \gamma\left\{3\delta_m^2 + b^2 - \frac{a}{\ln(T_S/T_R)_{\delta_m}}\right\} +$$

$$\left\{2\delta_m^3 + \delta_m b^2(1 + \varepsilon^2) - \frac{a(1-\alpha)\delta_m}{\ln(T_S/T_R)_{\delta_m}}\right\} = 0$$

Consideration of relative magnitudes in the first equation shows that the controlling terms are $(1 - \alpha)$ and $(\varepsilon^2 - \alpha)$. Since both ε and α are nearly unity in most practical problems, and since they must be determined

experimentally, there is little hope for getting accurate values of any one of α, ε, or γ from points on the residual curve, with or without measured values of the other two. Some experimental tests were made on solutions of $CHCl_3$ in CS_2, which confirmed the difficulty of properly extracting the information inherent in the residual curve. Attempts to calculate the frequency shift γ by solution of the quadratic in the second equation bore little relation to the measured shift.

If applications should arise where α and ε could be considered as unity with high accuracy, then the further condition $\gamma << \delta_m$ leads to an approximate relation

$$\gamma \longrightarrow \frac{8b^3}{3\sqrt{3}\,a} \cdot \ln\left(\frac{T_S}{T_R}\right)\delta_m$$

which is easily shown to be valid within 5% for $\gamma < b/3$, or within 0.5% for $\gamma < b/6$. Under these conditions it can be demonstrated that frequency shifts of 0.15 cm^{-1} in bands having a halfwidth of about 10 cm^{-1} should be measurable to about 25% accuracy. It is doubtful whether shifts of 2 cm^{-1} can be measured with this accuracy by direct measurement using commercial spectrometers.

The residual curves just discussed had not been mentioned in the literature at the time these calculations were carried out. Since that time Greinacher, Luttke, and Mecke (22) have described them, and have claimed for them great usefulness in measuring small frequency shifts. Their method of calculation was not given, and a search of the literature did not reveal any subsequent publication. The observations and calculations of the present work make it obvious that several difficulties stand

in the way of extracting the very detailed information present in the residual curves. In the first place, the occurrence of Lorentz or Gaussian band shapes is by no means universal (6); asymmetry and shape changes with concentration are quite common. The demonstrated sensitivity of the residual curve to all three band parameters, together with the ordinary limits of measurement and the fact that all three parameters tend to be concentration-dependent, greatly prejudice the accuracy of determinations, even where the band is truly symmetrical. This is not to say that these difficulties cannot be overcome; residual curves may yet prove a useful source of information in spectrometric studies.